

**ISTANBUL TECHNICAL UNIVERSITY ★ GRADUATE SCHOOL OF SCIENCE**  
**ENGINEERING AND TECHNOLOGY**

**ESTIMATION OF OPTIMUM BOREHOLE POINTS USING SOFTWARE  
SOLUTIONS**

**M.Sc. THESIS**

**Fariz NAHMATOV**  
**(505131003)**

**Department of Mining Engineering**  
**Mining Engineering Programme**

**Thesis Advisor: Assoc. Prof. Dr. Deniz TUMAÇ**

**AUGUST 2015**



**İSTANBUL TEKNİK UNİVERSİTESİ ★ FEN BİLİMLERİ ENSTİTÜSÜ**

**YAZILIM ÇÖZÜMLERİNİ KULLANARAK OPTİMUM SONDAJ  
NOKTALARININ BELİRLENMESİ**

**YÜKSEK LİSANS TEZİ**

**Fariz NAHMATOV**

**(505131003)**

**Maden Mühendisliği Anabilim Dalı**

**Maden Mühendisliği Programı**

**Tez danışmanı: Doç. Dr. Deniz TUMAÇ**

**Ağustos 2015**







**Fariz Nahmatov**, a **M.Sc.** student of ITU **Graduate School of Mining Engineering** with a student ID of **505131003**, successfully defended the **thesis** entitled **“ESTIMATION OF OPTIMUM BOREHOLE POINTS USING SOFTWARE SOLUTIONS”** which he prepared after fulfilling the requirements specified in the associated legislations, before the jury whose signatures are below.

**Thesis Advisor:**      **Assoc. Prof. Dr. Deniz TUMAÇ** .....

Istanbul Technical University

**Jury Members :**      **Assoc. Prof. Dr. Hakan TUNÇDEMİR** .....

Istanbul Technical University

**Assist. Prof. Dr. Murat YILMAZ** .....

Istanbul University

**Date of Submission: 13 July 2015**

**Date of Defense : 10 August 2015**





## **FOREWORD**

I have started my master study in Mining department as a scholar of SOCAR (State Oil Company of Azerbaijan Republic). Based on main interests of the company, it was mutually decided to work on this thesis topic. Therefore, I took my selective courses from Petroleum department.

The present study is a practical estimation of borehole coordinates for the geothermal field. Existing data was an indication of geothermal field in the subsurface. The research was done about the field of interest in terms of geology and topography. Moreover, several geophysical exploration methods were applied to detect the water zones. In this study, all geological and geophysical information were used to make an estimation about the target depth. Water zones and dominant faults were defined based on geophysical measurement. Eventually, all data used in Mining softwares to make a significant estimations for accurate interpretation. Finally, one point of the field was suggested to drill exploration well.

I place on record, my sincere thank you to the people who contributed of this study. I want to thank Dr. Deniz TUMAÇ, Associated Professor in Mining Faculty of Istanbul Technical University. I am extremely thankful and indebted to him for sharing expertise, and sincere and valuable guidance and encouragement extended to me. I also want to thank to Promete Company's all geology team members, owner Mr. İhsan YÜMLÜ for their assistance and contribution of this study. I am also grateful to Prof. Dr. Ali KOÇYİĞİT, and Geological Engineer Ms. Ceyda TUMAÇ for their knowledge sharing and support.

August 2015

Fariz NAHMATOV



## TABLE OF CONTENTS

	<u>Page</u>
<b>FOREWORD</b> .....	<b>VII</b>
<b>TABLE OF CONTENTS</b> .....	<b>IX</b>
<b>ABBREVIATIONS</b> .....	<b>XI</b>
<b>LIST OF TABLES</b> .....	<b>XIII</b>
<b>LIST OF FIGURES</b> .....	<b>XV</b>
<b>SUMMARY</b> .....	<b>XVII</b>
<b>ÖZET</b> .....	<b>XIX</b>
<b>1. INTRODUCTION</b> .....	<b>23</b>
<b>2. LITERATURE REVIEW</b> .....	<b>25</b>
2.1 Renewable Energy .....	26
2.1.1 Hydropower .....	29
2.1.2 Wind energy .....	30
2.1.3 Bioenergy .....	31
2.1.4 Solar energy .....	32
2.1.5 Geothermal energy .....	33
2.2 Geothermal Potential in Turkey .....	38
2.3 Exploration and Drilling .....	39
2.4 Using Methods .....	40
2.4.1 Dry steam .....	40
2.4.2 Flash steam .....	41
2.4.3 Single flash .....	41
2.4.4 Multiple flash .....	42
2.4.5 Binary .....	43
<b>3. GEOLOGICAL CONDITION OF THE FIELD</b> .....	<b>45</b>
3.1. General Stratigraphy of the Honaz-Kaklık Graben .....	45
3.1.1 Honaz shale .....	45
3.1.2 Yılanlı and Zeybekölentepe formations .....	47
3.1.3 Gereme and Çatalcatepe formations .....	49
3.1.4 Dereçiftlik group .....	49
3.1.5 İncesu formation .....	49
3.1.6 Denizli group .....	50
3.2. Structural Geology and Active Tectonics .....	51
3.2.1 Honaz fault .....	52
3.2.2 Aşağıdağdere fault zone .....	52
3.2.3 Şahinler fault zone .....	53
3.2.4 Küçükmalıdağı fault zone .....	53
3.2.5 Acıdere and Elmalı fault zone .....	54
3.2.6 Çaykaradere fault segment .....	54
<b>4. FIELD STUDIES</b> .....	<b>55</b>
4.1 Selection of Sample Points and Their Characteristics .....	56
4.2 Hot Water Points .....	56

4.3 Hydrochemistry.....	59
4.4 Gravity and Magnetic Method .....	59
<b>5. SOFTWARE SOLUTIONS FOR OPTIMUM BOREHOLE POINTS .....</b>	<b>71</b>
<b>6. CONCLUSION.....</b>	<b>79</b>
<b>7. RECOMMENDATION .....</b>	<b>85</b>
<b>REFERENCES .....</b>	<b>87</b>
<b>CURRICULUM VITAE .....</b>	<b>91</b>

## **ABBREVIATIONS**

<b>°C</b>	: Degrees Celsius
<b>CHG</b>	: Greenhouse Gas
<b>DDP</b>	: Deep Drilling Projects
<b>EJ</b>	: Exajoules
<b>ESG</b>	: Enhanced Geothermal System
<b>GHP</b>	: Geothermal Heat Pumps
<b>GW</b>	: Gigawatt
<b>IPCC</b>	: Intergovernmental Panel on Climate Change
<b>kW</b>	: Kilowatt
<b>LCA</b>	: Life Cycle Assessment
<b>LCOE</b>	: Levelized Costs of Electricities
<b>LCOH</b>	: Levelized Costs of Heat
<b>MT</b>	: Magnetotellurics
<b>MTA</b>	: Maden Teknik Aramaları Enstitüsü (General Directorate Of Mineral Research and Exploration)
<b>MW</b>	: Megawatt
<b>ORC</b>	: Organic Rankie Cycle
<b>R&amp;D</b>	: Research and Development
<b>RE</b>	: Renewable Energy
<b>RPS</b>	: Renewable Portfolio Standards



## LIST OF TABLES

	<b><u>Page</u></b>
<b>Table 4.1:</b> Coordinates and parameters of 22 sample points of the field (Yüksel, 2013). .....	58
<b>Table 5.1:</b> Estimation of temperature in certain depth based on geothermal gradient. ....	72
<b>Table 5.2:</b> Descriptive statistic for temperature. ....	72
<b>Table 6.1 :</b> Average temperature and elevation of water zones .....	80
<b>Table 6.2:</b> Optimum wellbore coordinates .....	83





## LIST OF FIGURES

	<u>Page</u>
<b>Figure 2.1:</b> Shares of energy sources in total global primary energy supply in 2008 (Edenhofer et al., 2012).....	26
<b>Figure 2.2:</b> Total World Energy Consumption by Source (2013) (Url-1) .....	26
<b>Figure 2.3:</b> Illustrative paths of energy from source to service. All connected lines indicate possible energy pathways (Edenhofer et. al, 2012). .....	29
<b>Figure 2.4:</b> Geothermal electric installed capacity by country in 2009. ....	38
<b>Figure 2.5:</b> Main geothermal fields of Western Anatolia (Şimşek, 2014). .....	39
<b>Figure 2.6:</b> Dry steam method (Url-2). ....	41
<b>Figure 2.7:</b> Flash steam method (Url-2). .....	42
<b>Figure 2.8:</b> Binary Cycle (Url-2). .....	43
<b>Figure 3.1:</b> Simplified tectonic map showing the location of Turkey and its surroundings in terms of plate tectonic and important plate boundaries (Koçyiğit, 2013). ....	46
<b>Figure 3.2:</b> Generalized tectonic-stratigraphic vertical section of the Honaz-Kaklık Graben and its surroundings (Koçyiğit, 2013). .....	48
<b>Figure 4.1:</b> Overview of the investigated field. ....	56
<b>Figure 4.2:</b> Bouguer Gravity (Red.Den.:2.30 g/cm <sup>3</sup> ) (Yüksel, 2013). .....	65
<b>Figure 4.3:</b> Isostatic effect on the field (Yüksel, 2013). ....	65
<b>Figure 4.4:</b> Isostatic Gravity of the field (Yüksel, 2013). ....	66
<b>Figure 4.5:</b> Gravity measurement in target depth (Yüksel, 2013). ....	66
<b>Figure 4.6:</b> Regional Faults for -2500 meter depth. ....	67
<b>Figure 4.7:</b> Regional Dominant Faults for -2500 meter depth. ....	68
<b>Figure 4.8:</b> Vertical Magnetic intensity (Yüksel, 2013). ....	69
<b>Figure 4.9:</b> Analitical Signal of Vertical Magnetic (Yüksel, 2013). .....	69
<b>Figure 5.1:</b> Variogram analysis for modelling (GS+). ....	75
<b>Figure 5.2:</b> Variogram values and model selection. Spherical model is most suitable for the case (GS+). ....	75
<b>Figure 5.3:</b> Heat distribution for the field. Derived from GS+ with Kriging, and visualized in Micromine software. ....	76
<b>Figure 5.4:</b> Water zones and faults in heat distribution map. ....	77
<b>Figure 6.1:</b> Merged coordinates of hot water reserves versus heat distribution of the field. ....	80
<b>Figure 6.2:</b> Nearest surface points to the water zones. ....	81
<b>Figure 6.3:</b> Suggested water zones marked on topography. ....	83



# **ESTIMATION OF OPTIMUM BOREHOLE POINTS USING SOFTWARE SOLUTIONS**

## **SUMMARY**

Nowadays, increment in population, industrial developments, life style of people, and technological progresses lead to rise in demand for energy sharply. It is obvious that 60% of the energy share belongs to fossil fuels reserves. Conventional methods are major systems that create pollution for environment. Besides, the reserves will be come to an end in a certain time of period.

Developed countries are now using renewable energy methods such as hydraulic, wind, geothermal, biomass, solar energy, hydrogen based energy, wave energy on conducive to produce energy. Mostly those sources are beneficial for electrical energy. The energy demand of Turkey, one of the developing country, is increasing with rise of economy, population, industry, and consumption of resources. Turkey's foreign based energy dependent rate is 72%. In one hand the exploration of fossil fuels, in other hand defining potential of the renewable energy resources works are carrying out.

Turkey is situated in the place of formation of Alp and Himalayas mountain belts. Very fractured structure while gained young tectonic period indicates that this region is rich of geothermal resources. The geothermal heat potential of Turkey is considered about 31.500 MW thermal. The first exploration in this country was started 45 years ago by General Directorate of Mineral Research and Exploration (MTA). 190 geothermal fields have been discovered until today during exploration work. The shares of the discovered field are given below. 79% in Western Anatolia, 8.5% of Central Anatolia, 7.5% in Marmara region, 4.5% in Eastern Anatolia, and 0.5% other.

In exploration of geothermal field, geological, geophysical, geochemical, and drilling study should be carried on. These particular studies can be summarized with specific headings. To figure out of the lithological, stratigraphical, petrographical parameters of the field in terms of geology; to examine geophysical properties such as subsurface geophysics; to learn geological, tectonic, and lithological properties with the help of photogeology studies; To examine water chemistry with geochemical studies; To get acquainted with subsurface geology, hydrothermal geology, alteration zones, reservoir, cap rock's properties, lithological-stratigraphic and hydraulic properties of the formation with the help of drilling work.

In this study, geothermal exploration work is investigated for an area located between Honaz-Kaklık and Acıgöl grabens. General geological stratigraphy and active faults in the field were investigated by the company in the area licensed. From 22 points hot water and cold water samples were taken. The major analyses were executed by the company as anion-cation analysis and heavy metal analysis. Hereby data which contains pH, electric current, and petrophysical parameters were obtained to create a database. The heat estimation was obtained for the target zone that considered existence of water in particular depth -2500 m.

The target depth was investigated in terms of geology and stratigraphy of the field. Denizli group has green yellow red shale, limestone, and dolomite. This type of formations has no permeability although they have porous rock. Rock that has no

permeability, considered cap rock for the reservoir. That is why the depth of this rock group became a target depth for this field. Below this rock group there is porous, high permeable limestone which regarded sufficient reservoir to start a production.

Nonetheless, based on geothermal gradient for the region was used for getting accurate result. Heat data that got from 22 sample points were used in Geostatistical program (GS+) in order to make estimation in terms of heat temperature, more than 60000 data were obtained. Considering Micromine software advantage in drawing more accurate graphic, data from Geostatistic program were used in Micromine program. The resultant graph's uncertainties were mentioned on the interpretation part. The field has certain water zones, and the resultant graph cannot be applied for all area since dominant faults were not used as a parameter in the softwares. It is obvious that presence of water depends on presence of faults and their structure. That is why the main investigation was based on the gravity and magnetic study was done by the company which was very costly. Obtained new data merged with data received from mining softwares (GS+, and Micromine) so that the more accurate temperature distribution was obtained at the end. Consequently, 3 drilling target coordinates were proposed, and their advantages and disadvantages were interpreted.

Surely, the result of the geostatistical approach might be discussed. There is a necessity of more input parameter to increase accuracy of results. In this study, the availability of getting accurate result of optimum borehole coordinate was checked with the limited drilling data. The exploration optimum borehole coordinate could be obtained with MT (Magnetotelluric) method which is very expensive. However in the further stages results might be checked with MT method.

In this study, the input parameters were selected for softwares. Numerical input values were correlated in terms of geology, lithology, and temperature. During software application, the only parameter used as an input was temperature. Since the study was focused on first exploration well to start drilling and test the reservoir. Temperature of the target depth were much significant on this stage. For instance temperature distribution data were sufficient to make a modeling on mining software as GS+. The only disadvantage were number of data provided from surface. However,  $r^2$  value for modeling was 87% which can be considered sufficient for kriging application. In last section of the study contains suggestions for further work. For instance after every new exploration or production well new data will be added as an input. The software application might be rerun after every new data input to decrease uncertainty of the result.

## YAZILIM ÇÖZÜMLERİ KULLANILARAK OPTİMUM SONDAJ NOKTALARININ BELİRLENMESİ

### ÖZET

Günümüzde hızlı artan nüfus ve endüstriyel gelişmeler, insanların refah seviyesinin yükselmesi ve teknolojik gelişmeler ile gün geçtikçe enerji gereksinimine olan talebi artırmaktadır. Dünya’da enerji üretim miktarı incelendiğinde neredeyse % 60 ile en büyük payı fosil kaynaklı yakıtların aldığı görülmektedir. Geleneksel enerji üretim yöntemleri çevre kirliliğinin en önemli nedenlerinden biridir. Ayrıca, fosil yakıtların yakın zamanda tükeneceği de bilinmektedir.

Gelişmiş ülkelerde yenilenebilir enerji kaynakları olarak bilinen hidrolik, rüzgar, jeotermal, biyokütle, güneş, hidrojen, dalga vb. enerji kaynaklarından başta elektrik üretimi olmak üzere yararlanılmaktadır. Gelişmekte olan bir ülke olan Türkiye’nin de artan nüfus ve büyüyen ekonomisine paralel olarak enerji kaynakları tüketimi her geçen gün artmaktadır. Türkiye’nin enerji yapısı % 72 oranında dışa bağımlıdır. Bu oranı azaltabilmek için bir yandan fosil enerji hammaddesi arama çalışmaları yürütürken, diğer yandan da yenilenebilir enerji kaynaklarının potansiyelinin belirlenmesi ve kullanımı çalışmaları devam etmektedir.

Jeolojik olarak Alp-Himalaya dağ oluşum kuşağında yer alan Türkiye, genç tektonik dönemde kazanmış olduğu çok kırıklı yapısı ve geçirmiş olduğu volkanik faaliyetlerden dolayı jeotermal kaynaklar yönünden zengin konumdadır. Ülkemizin jeotermal ısı potansiyeli yaklaşık 31,500 MW termal olarak kabul edilmektedir. Türkiye’de jeotermal enerji çalışmaları yaklaşık 45 yıl önce Maden Tetkik Arama (MTA) Genel Müdürlüğü tarafından başlatılmıştır. Bugüne kadar yapılan çalışmalarla yaklaşık 190 adet jeotermal alanın varlığı keşfedilmiştir. Bu alanların % 79’u Batı Anadolu’da, % 8,5’i Orta Anadolu’da, % 7,5’i Marmara Bölgesinde, % 4,5’i Doğu Anadolu’da ve % 0,5’i diğer bölgelerde yer almaktadır.

Jeotermal enerji potansiyelinin araştırmalarında, sahanın ayrıntılı jeolojik, jeofiziksel, jeokimyasal ve sondaj çalışmalarının yapılması gerekmektedir. Bu detaylı çalışmalar kısaca şu başlıklar altında özetlenebilir: Jeolojik çalışmalar ile formasyonların litolojik, stratigrafik, petrografik ve jeolojik incelemelerinin yapılması; Jeofizik çalışmalar ile yeraltı jeolojisinin incelenmesi; Fotojeolojik çalışmalar ile jeolojik, tektonik ve litolojik özelliklerin incelenmesi; Jeokimyasal çalışmalar ile su kimyasının incelenmesi; Sondaj çalışmaları ile yeraltı jeolojisi, hidrotermal alterasyon zonları, hazne ve örtü kayaların özellikleri, formasyonların litolojik-stratigrafik ve hidrolik özelliklerinin incelenmesi.

Bu çalışma kapsamında, Honaz-Kaklık ve Acıgöl Grabenleri arasında yer alan lisanslı bir saha üzerinde yapılan jeotermal arama çalışmaları incelenmiştir. Lisanslı firma tarafından gerçekleştirilen bölgenin genel jeolojisi-stratigrafisi ve aktif fay yapısı ile ilgili raporlar detaylıca incelenmiştir. Lisanslı ruhsat sınırları içerinden

farklı 22 noktadan sıcak ve soğuk su örnekleri alınmıştır. Alınan bu örnekler üzerindeki yüksek maliyetli olan major anyon ve katyon analizleri, izotop analizleri ve ağır metal analizleri ilgili lisanslı firma tarafından yaptırılmıştır. Böylelikle veri tabanımızda kullanılacak olan su sıcaklığı, pH ve elektriksel iletkenlik gibi fizikokimyasal parametreler elde edilmiştir. Jeotermal rezervuarın olma olasılığının bulunduğu -2500 m derinlik için bölgenin jeotermal gradyan özellikleri göz önünde tutularak su sıcaklık tahminleri yapılmıştır.

Hedef alınmış derinliğin jeolojisi incelenmiştir. Denizli grubunda bulunan yeşil, kırmızı, sarı kil, kireçtaşı ve dolomit genellikle gözenekli kayalar türleridir. Kayaçlarda bulunan gözenekler birbirleriyle bağlantılı olmadıkları için bu kaya grubunun geçirgenliği sıfıra yakındır. Geçirgenliği olmayan kayalar da örtü kaya olarak kabul edilir ve hedef derinlik buna göre belirlenir. Bu araştırmada da Denizli grubun özellikleri hedef derinliğinin belirlemeye yardım etmiştir.

22 noktanın -2500 m derinliği için elde edilen sıcaklıklar, jeostatistiksel (GS+) program yardımıyla ruhsat sınırı içinde 60,000'den fazla noktanın sıcaklık tahmini yapılmıştır. Jeostatistiksel yaklaşımda kullanılan metot kriging metodudur. Bu metot bilinmeyen noktaya olan komşu noktaların ağırlıklı ortalamalarını kullanarak istatistiksel tahmin yapmaktadır. Böylece, 22 noktanın verilerini kullanarak bu noktalar arasında kalan binlerce nokta bu yaklaşım kullanılarak tahmin edilmiştir. Bu tahminlerin veri azlığından ötürü belirsizliği vardır. Fakat, bu belirsizliği her yeni kuyu açıldığında, yeni veriler ekleyerek azaltmak mümkündür. Bundan başka söz konusu su sıcaklığı olduğu için belirsizlik oranı biraz düşmektedir. Isı transferini ve suyun mevcut ısını etrafına dağıtma şekli göz önüne alındığında, ısı dağılımı haritasının kullanılabileceği bilinmektedir. Micromine programının grafik çizimindeki avantajını göz önüne alarak ısı haritası oluşturulmuştur. Elde edilen grafiklerde düzeltmeye gidilmesinin gerekli olduğu belirlenmiştir. Çünkü sahanın baskın fay yapısı bu programda kullanılamamıştır. Fayların olduğu bölgelerde sıcak su olma olasılığının yüksek olduğu bilinen bir gerçektir. Bu sebepten ötürü; lisanslı firma tarafından yüksek maliyetler ödenerek yaptırılan gravite-manyetik çalışmaları esas alınmıştır. Elde edilen yeni verilerden yola çıkılarak GS+ programıyla tahmine geri dönmüştür. Böylece, lisanslı saha için daha gerçekçi bir ısı dağılımı elde edilmiştir. Sonuç olarak, bölgede jeotermal arama yapılabilmesi için 3 sondaj noktası önerilmiştir ve her birinin avantajlı ve dezavantajlı tarafları belirtilmiştir.

İlk açılacak olan sondaj kuyusunda test etmeden önce, bazı log çalışmalarının yapılması önerilmiştir. Bu log çalışmalarında sahanın belirli derinliklerinde olan kayalar türleri hakkında daha fazla bilgi edinebilir. Bundan başka, kuyu logunun yardımı ile kil ve sondaj sırasında ortaya çıkabilecek riskleri de ortaya çıkarılabilir. Logun en önemli avantajı ise öz direnç loglarının sondaj noktasının belirli bir çevresinin elektrik dayanıklılığını ölçmesidir. Elektrik dayanıklılığını belirlemekle, yalnızca kuyunun olduğu yerde değil, kuyunun yüzmetrelerce ilerisindeki yeraltı sularını, ve suların sıcaklığını belirlemekte mümkündür.

Bu çalışmaların güvenilirliği elbette ki tartışılabilir. Güvenirliği artırmak için daha çok girdi parametresine ihtiyaç vardır. Bu çalışma, sondaj noktası tahmini için kısıtlı verilerden sonuca ulaşıp ulaşılmayacağını incelemektir. Gerçekçi sondaj noktasına MT yöntemi ile daha kolay ulaşılabilir, fakat bu yöntem pahalıdır. Elde edilen sonuçların doğruluğu MT yöntemi ile test edilebilir.

Bu çalışmada kullanılan GS+ ve Micro-mine yazılımlarının girdi parametreleri var olan veri tabanından seçilmiştir. Sayısallaştırılan değerlerde kabuller yapılmıştır. Her

yapılan kabul, jeolojinin karmaşıklığı göz önünü alındığında bir bölgeden diğer bölgeye farklılık gösterebilir.





## **1. INTRODUCTION**

By 1920, energy requirement doubled with development of the industry in the world. By that time, rising of the global population, and consumption rate increased the energy demand. Life standards had been changed with development of the technology, engineering, and economy. All aspects mentioned above, claimed the energy industry to provide more energy every decades. Therefore, energy companies started produce more energy such as hydrocarbon, coal, and other fossil fuel production. Fossil fuels are organic substances that formed in million years by natural processes of dead organism. In the past, fossil fuels such as oil and natural gas were used for heating. Development of the engine industry affected all transport manufacturing companies. The development of petroleum industry nearly ended the sail boat field. Engine revolution applied to ship building industry and this was also beginning of the air business. The petroleum industry was leading field for energy. However, in the late 1990's world environment affected from excessively using of hydrocarbons in all fields. The consequence of this carbon dioxide emission was global warming has been started, and indicates its unfavorable effects to the earth. This outcome lead world to face challenges in decreasing of using hydrocarbon energies, and to explore and produce green energy for the earth. Surely, it is impossible to decrease demand with increasing population, but it is possible to develop renewable energy industry and science. Hence in last two decades were inception of some industries and field of studies (Edenhofer et al., 2012).

Climate change is one of the significant challenges of this century. Major severe impacts might still be avoided if efforts are made to convert current energy systems. Renewable energy sources have a crucial potential to dislocate emissions of greenhouse gases from the combustion of fossil fuels and thereby to mitigate climate change. If applied properly, renewable energy sources could conduce to social and economic development, to energy accession, to a reliable and sustainable energy supply, and to a decrease of negative effect of energy provision on the environment and human health (Edenhofer et al., 2012). All societies need energy duties such as

cooking, lighting, communication, comfort, mobility, transportation and etc. World is challenging to develop use of renewable energy, and enhance its engineering and technology side.

In this study, geothermal field study work carried on Honaz Kaklık region. The study were contained of geological research, geophysical applications, and mining software applications. In the first stage of the study, general geology and stratigraphy were researched. After this research detailed stratigraphy and lithology of the field were analyzed based on the rock type in terms of density porosity and permeability. Thence the less permeable lithology obtained which indicates cap rock for the reservoir. Denizli group rocks are highly porous. However rock's pores sizes are not connected. Hence rocks are not permeable. The average depth of this group is 2500. Target depth was obtained from geological research. Gravity and magnetic measurement work carried by Promete Company. Interpretation of gravity density differences, dominant and regional faults were explored. Magnetic anomalies and obtained fault map by gravity measurement helped to identify water zones in the field. There are 22 hot water points on the surface. In this study the only characteristic used in estimation stage which is temperature of water. Using geothermal gradient for the region 22 points temperature were estimated in 2500 meter depth. Obtained 22 temperature data on particular depth were used to make descriptive statistic and kriging on GS+ software. Software resulted 60,000 data out 22 data. Data obtained from kriging application used on Micromine software in order to make graph. Heat distribution graph map merged with water zone map that obtained from gravity and magnetic measurement. Average temperature were estimated for each water zones using merged graph. As a result 3 water zones were suggested for starting exploration taking into account average temperature of water zone, and elevation of surface. Eventually, as a recommendation, the particular logging work as sonic log, and resistivity log were proposed for increasing accuracy of the estimation.

## 2. LITERATURE REVIEW

Sometimes it is called alternative energy sources, being environmental friendly. Here we can find statistic of energy consumption. Renewable energy provided an estimated 19% of global final energy consumption in 2012, and continued to grow in 2013. Of this total share in 2012, modern renewables accounted for approximately 10%, with the remainder (estimated at just over 9%) coming from conventional biomass. Heat energy from modern renewable sources accounted for an estimated 4.2% of total final energy use; hydropower made up about 3.8%, and an estimated 2% was provided by power from wind, solar, geothermal, and biomass, as well as by biofuels. (Zervos, 2014). Although world used to live on with fossil fuels fully, today, it is been more than 10% part of energy supplement is provided by renewable energy. In Figure 2.1 we can see the statistic of energy sources in 2014. The Figure 2.2 shows the energy consumption with categories in all over the world. There are plenty of research on environmental effect of energy sources. Majority of them analyze supply and consumption rates of energy in the world for today and historical base. In recent years the increase of atmospheric concentration of CO<sub>2</sub> resulting from increased consumption of fossil fuels has become an international concern. In examining global energy use, it is useful to include in out accounting the concomitant CO<sub>2</sub> emission to provide a perspective on the problem of managing the potential threat of global climate change resulting from these emissions. Currently, universal carbon emissions amount to approximately 7.8 GT C/y (to obtain CO<sub>2</sub> emissions, multiply by 44/12, the molecular weight ration of CO<sub>2</sub> and C). In terms of absolute quantities, the United States and China are the largest emitters of carbon, with 1.57 and 1.66 Gt C/y respectively followed by Russia with 0.43 Gt C/y (Fay, 2012).

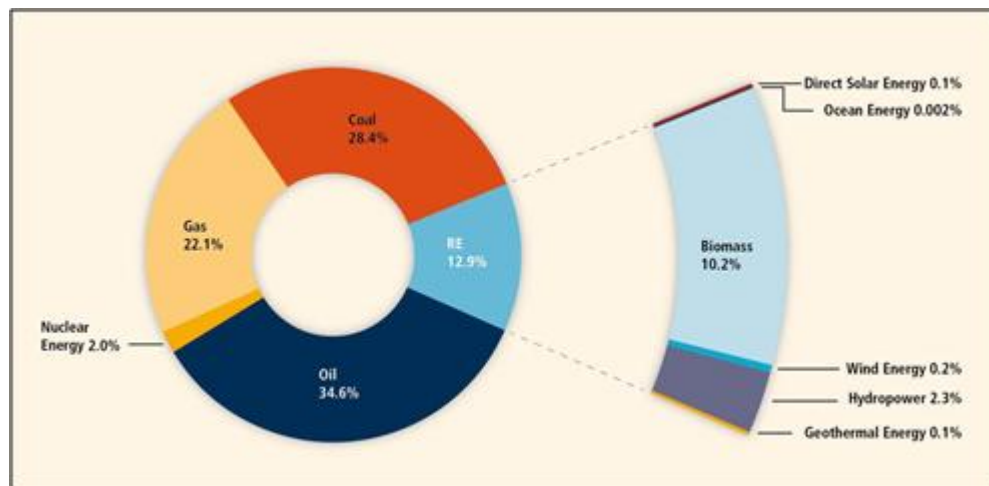


**Figure 2.1:** Shares of energy sources in total global primary energy supply in 2008 (Edenhofer et al., 2012).

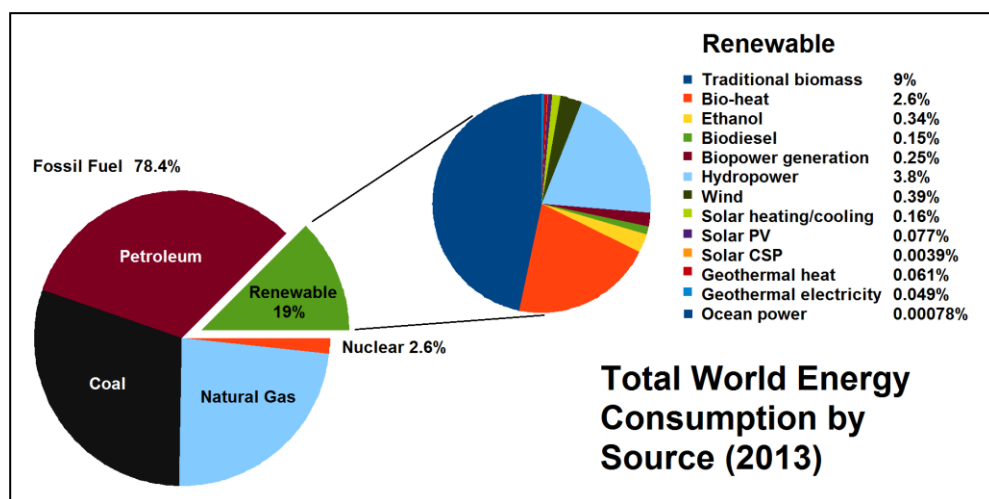


**Figure 2.2:** Total World Energy Consumption by Source (2013) (Url-1)

## 2.1 Renewable Energy

Renewable energy sources play a major role in providing energy facilities in a sustainable manner and, in particular, in justifying climate change. Renewable Energy Sources and Climate Change Mitigation discovers the current contribution and potential of renewable energy (RE) sources to offer energy facilities for a sustainable social and economic development pathway. It includes calculations of available RE resources and technologies, costs and co-benefit, barriers to up-scaling and integration necessities, future scenarios and policy choices. Greenhouse gas (GHG) emissions associated with the provision of energy services are a main cause of climate change. The Intergovernmental Panel on Climate Change (IPCC) decided

that “Most of the observed upsurge in global average temperature since the mid-20th century is possible due to the experiential increase in anthropogenic greenhouse gas concentrations” (Edenhofer et al., 2012).

Concentrations of CO<sub>2</sub> have been continued to raise and by the end of 2010 had extended 390 ppm CO<sub>2</sub> or 39% above preindustrial levels. The longstanding baseline scenarios was reviewed for the AR4 show that the anticipated reduction in the energy intensity will not be able to satisfy for the effects of the projected increase in the global gross local product. As a result, most of the circumstances exhibit a strong surge in key energy supply throughout this century. In the absence of any climate policy, the crushing majority of the baseline scenarios show much higher emissions in 2010 compared to 2000, suggesting rising CO<sub>2</sub> concentrations and, in turn, boosted global warming. Depending on the fundamental socioeconomic scenarios and taking into account extra uncertainties, worldwide average temperature is expected to increase and to reach a level between 1.1°C and 6.4°C over the 1980 to 1999 usual by the end of this century. To escape adverse impacts of such climate change on water resources, ecologies, food security, human health and coastal settlements with possibly permanent abrupt changes in the climate system, the Cancun Agreements encourage for limiting global average temperature increases to no more than 2°C above preindustrial values, and decided to consider limiting this growth to 1.5°C. In order to be confident of reaching a balance temperature rise of only 2°C to 2.4°C, GHG concentrations would need to be calmed in the range of 445 to 490 ppm CO<sub>2</sub> eq in the atmosphere. There are numerous means for dropping GHG emissions from the energy system, while still supplying desired energy services. RE technologies are varied and can make a service the full range of energy service needs. Various types of RE can supply electricity, thermal energy and mechanical energy, as well as produce fuels that are able to satisfy multiple energy service needs. RE is any method of energy from solar, geophysical or biological sources that is refilled by natural processes at a rate that equals or exceeds its rate of use. Unlike fossil fuels, most forms of RE are produced slight or no CO<sub>2</sub> emissions. The role RE will offer within the collection of low carbon technologies greatly depends on the economic competition between these technologies, their relative ecological burden (beyond climate change), as well as on safety and societal sides. An all-inclusive assessment of any collection of mitigation choices would involve an assessment of

their respective mitigation potential as well as all related risks, costs and their input to sustainable development. Even without a drive for climate change mitigation, situations that are 165 studied find that the growing demand for energy services is likely to drive RE to levels above today's energy usage. On a global level, it is estimated that RE accounted for 12.9% of the total 492 EJ of main energy supply in 2008. The largest RE share was biomass (10.2%), with the common (approximately 60%) of the biomass fuel used in conventional cooking and heating applications in developing countries, however with quickly growing use of modern biomass as well. Hydropower represented 2.3%, whereas other RE sources calculated for 0.4%. In 2008, RE donated roughly 19% of global electricity supply (16% hydropower, 3% other RE), biofuels donated 2% of global road transport fuel supply, and conventional biomass (17%), modern biomass (8%), solar thermal and geothermal energy (2%) together fuelled 27% of the total global need for heat. The contribution of RE to main energy supply differs substantially by country and region. Situations of future low greenhouse gas futures consider RE and RE in combination with nuclear, and coal and natural gas with carbon capture and storage. While the RE share of global energy using is still comparatively minor, deployment of RE was increasing quickly in last years. Of the around 300 GW of new electricity generating capacity added worldwide in two years from 2008 to 2009, 140 GW collected from RE additions. Jointly, developing countries hosted 53% of global RE power generation capacity in 2009. Under most circumstances, increasing the portion of RE in the energy mix will need policies to encourage changes in the energy system. Government policy, the falling cost of many RE technologies, changes in the charges of fossil fuels and other issues have supported the continuing rise in the use of RE. These developments propose the possibility that RE could play a much more significant role either in developed or developing countries in the coming decades. Some RE technologies can be distributed at the point of use in rural and urban areas, whereas others are mainly employed within huge (centralized) energy systems. Though many RE technologies are theoretically mature and are being distributed at important scale, others are in an earlier phase of technical maturity and profitable placement. The theoretical advantage for RE critically exceeds all the energy that is used by all economies on Earth. The worldwide technical potential of RE sources will not restrict continued market development. A varied range of approximations are provided in the literature but studies have dependably found that the total universal

technical capacity for RE is essentially higher than both current and predictable future worldwide energy need. The technical capacity for solar energy is the highest among the RE sources, but significant technical potential endures for all forms of RE. The total size of the global technical capacity for RE as a whole is unlikely to restrict RE placement. Every energy sources need multi-step procedure in order to be converted into kinetic energy. Figure 2.3 shows ways of energy from source to services possible energy pathways. The energy services delivered to the users can be provided (Edenhofer et al., 2012).

World's situation challenge the scientist to work on green energy more. Hence different branches of green energy are developing rapidly. In this section some information about every energy sources and its advantages will be given. The mainstream technologies for renewable energy are, wind power, hydropower, solar energy, biomass, biofuel, geothermal energy.

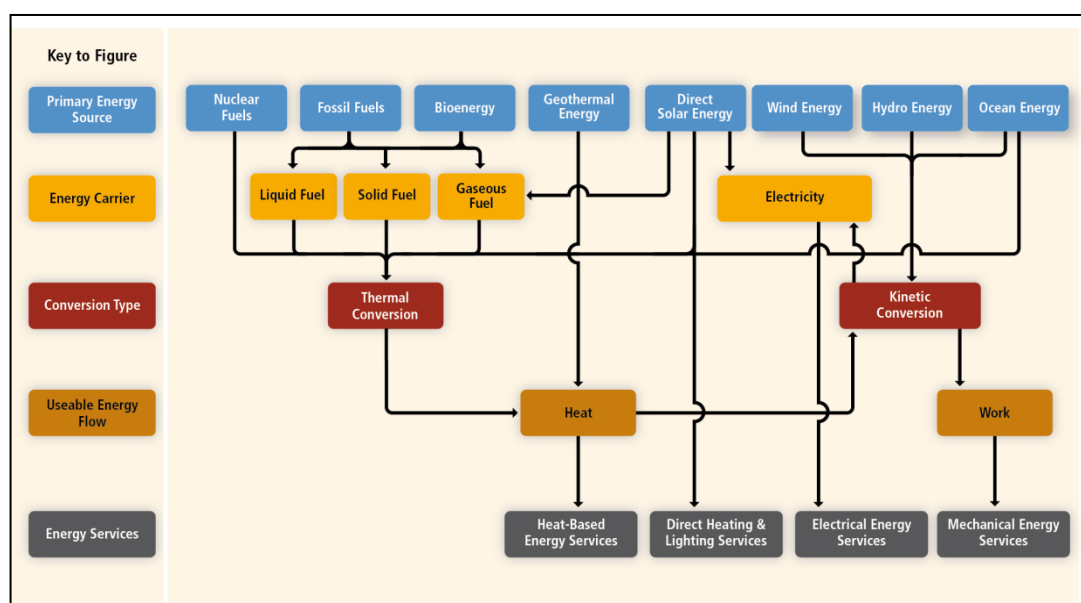


**Figure 2.3:** Illustrative paths of energy from source to service. All connected lines indicate possible energy pathways (Edenhofer et. al, 2012).

### 2.1.1 Hydropower

Global use of hydropower increased more than 5 percent between 2009 and 2010, according to new research published by the Worldwatch Institute for its Vital Signs Online publication. Hydropower use reached a record 3,427 terawatt-hours, or about 16.1 percent of global electricity use, by the end of 2010, continuing the swift rate of rise practiced between 2003 and 2009. The cost of hydropower is moderately low,

making it a competitive source of renewable power. The normal cost of electricity from a hydro plant larger than 10 megawatts is 3 to 5 U.S. cents each kilowatt-hour. Hydropower is an unsteady source of electricity since plants might be ramped up and down very easily to adapt to fluctuating energy demands. Yet there are many undesirable aspects related with hydropower: for example, damming interrupts the flow of rivers and may harm local ecologies, and building huge dams and basins frequently contains moving people and wildlife and needs substantial amounts of carbon-intensive cement. China was the major hydropower supplier and is expected to continue to lead global hydro use in the upcoming years. The country produced 721 terawatt-hours in 2010, representing around 17 percent of domestic electricity use. China also had the highest installed hydropower capacity, with 213 GW at the end of 2010. It added more hydro capacity than any other country, 16 GW in 2010, and plans to add 140 GW by 2015. This is corresponding to building about seven more dams the size of China's Three Gorges Dam, currently the largest in the world. Hydropower is produced in at least 150 countries but is concentrated in just a few countries and regions. The Asia-Pacific region generated roughly 32 percent of global hydropower in 2010. Africa produces the least hydropower, accounting for 3 percent of the world total, but is considered the region with the greatest capacity for increased production. In 2008, four countries—Albania, Bhutan, Lesotho, and Paraguay—generated all their electricity from hydropower, and 15 countries generated at least 90 percent of their electricity from hydro. Iceland, New Zealand, and Norway produce the most hydropower per capita. Micro-hydropower, which is defined as a plant with an installed capacity of 100 kilowatt (kW) or less, has grown in importance over the last decade and can be an effective means of providing electricity to communities far from industrial centers. As of 2009, approximately 60 GW of small hydro has been installed worldwide, accounting for less than 6 percent of the hydropower overall. Small hydro is possible to expand, specifically as overcrowded countries like India continue to maintain rural electrification (Kumar, 2013).

### **2.1.2 Wind energy**

When considering the installation of a wind farm, the single most important characteristic is the wind speed. With a doubling of average wind speed, the power in the wind increases by a factor of 8, so even small changes in wind speed can produce



large changes in the economic performance of a wind farm. By way of design, if the regular wind speed at a given site rises from 5 meters per second (m/s) to 10 m/s, the quantity of energy produced by a wind farm will rise by over 130%. Detailed and safe information about how powerfully and from which way the wind blows, and time, is therefore vital for any potential wind power development. First calculation of the wind resource accessible at a given site includes the study of data from near weather stations and professional computer software that is able to model the wind supply. To contribute in this process, national, regional and local “wind diagrams” was produced; an evaluation of European wind diagrams has been investigated. Although detail differs from region to region, the likely average wind speed in a given region. If the site has potential, more complete measurements are driven out through the erection of an anemometry pole, bearing a number of apparatus – anemometers – used in measuring wind speed and wind direction fitted at different elevations on the pole. Resource calculations are increasingly refined by analyzing restrictions as limited geography, economics, and alternative land use, to yield a “practical” resource. The exploitable onshore wind resource for the EU-25 is predictably projected at 600 TWh and the offshore wind resource up to 3,000 TWh; the higher end of this far exceeding the EU-15’s entire electricity usage. The European Wind Atlas produced by the Danish national research laboratory, promises a significant overview of the EU potential. An offshore type is also applicable. Although long period have accelerated, majority of European nations still have huge wind resources waiting to be used effectively. There is also significant potential in new member states and in Russia. Main report offer a selection of available onshore and offshore wind maps (Edenhofer et al., 2012).

### **2.1.3 Bioenergy**

Bioenergy has an important greenhouse gas (GHG) mitigation capacity, provided that the resources are industrialized sustainably and that efficient bioenergy systems are used. Certain present systems and crucial future choices counting perennial cropping systems, usage of biomass remains and wastes and advanced conversion systems are able to hand in of 80 to 90% emission drops compared to the fossil energy baseline. Yet, land use change and forest management that lead to a damage of carbon stocks (direct) in addition to indirect land usage modify effects can reduce, and in some cases more than deactivate, the net optimistic GHG mitigation

influences. Influences of climate change through temperature rises, rainfall pattern changes and increased regularity of dangerous events will effect and interact with biomass resource capacity. This mutual effect is not still understood, but it is possible to exhibit strong regional differences (Huertas et al., 2010). Climate change influences on biomass feedstock production occur but if global temperature increase is limited to less than 2°C compared with the pre-industrial record, it may strike an attitude few constraints. Merging adaptation procedures with biomass resource production may propose more stable opportunities for bioenergy and duable harvesting systems (Edenhofer et al., 2012).

#### **2.1.4 Solar energy**

Solar energy is abundant and proposes important potency for near-term (2020) and long-term (2050) climate change mitigation. There are a wide diversity of solar technologies of different maturities that can, in most areas of the world, conduce to a suite of energy services. Even though solar energy generation still only represents a small portion of total energy usage, markets for solar technologies are growing quickly. Much of the fascination of solar technology is its naturally smaller environmental load and the chance it offers for positive social effects. The cost of solar technologies reduced much over the past 30 years and technical advances and supportive public policies proceed to propose the potential for extra cost drops. Potential placement scenarios varies extensively from a marginal role of direct solar energy in 2050 to one of the key sources of energy supply. The real placement accomplished will hinge on the degree of continued innovation, cost drops and supportive public policies. Solar energy is the most generous of all energy resources. Truly, the rate at which solar energy is received by the Earth is around 10,000 times higher than the rate at which humanity consumes energy. Although not all countries are equally endowed with solar energy, signify cannot contribution to the energy mix from direct solar energy is likely for almost everywhere. Nowadays, there is no proof indicating a major impact of climate change on local solar resources. Solar energy transformation contains large family of different technologies capable of meeting a diversity of energy service needs. Solar technologies may send heat, cooling, natural lighting, electricity, and fuels for a host of applications. Transformation of solar energy to heat (i.e., thermal conversion) is comparatively elementary, because any physical object placed in the sun will absorb thermal energy. However, optimizing

that absorbed energy and hold it from escaping to the surroundings can take particular techniques and apparatus as evacuated spaces, optical coatings and mirrors. Which method is used depends on the application and temperature at that the heat is to be assigned. This might range from 25°C (e.g., for swimming pool heating) to 1,000°C (e.g., for dish/stirling concentrating solar power), and even up to 3,000°C in solar furnaces. Passive solar heating is a method for supplying comfortable conditions in houses by exploiting the solar flash event on the buildings through the use of glazing (windows, sun spaces, conservatories) and other transparent resources and handling heat gain and loss in the building without the main use of pumps or fans. Solar cooling for houses can also be reached, for instance, by using solar-derived heat to trigger thermodynamic cooling absorption or adsorption cycles. Solar energy for illumination truly needs no transformation since solar illumination occurs naturally in buildings through windows. However, maximizing the effect needs specialized engineering and architectural plan (Edenhofer et al., 2012).

#### **2.1.5 Geothermal energy**

Geothermal energy has the capacity to deliver longstanding, safe base-load energy and greenhouse gas (GHG) emissions drops. Available geothermal energy from the Earth's interior provides heat for direct use and to generate electric energy. Climate change is not likely to have any key impacts on the effectiveness of geothermal energy use, but the common placement of geothermal energy could play a significant role in mitigating climate change. In electricity applications, the commercialization and use of enhanced geothermal systems (EGS) can play a central role in creating the size of the contribution of geothermal energy to longstanding GHG emissions drops. The natural refill of heat from earth procedures and modern reservoir management techniques allow the sustainable use of geothermal energy as a low-emission, renewable resource. With suitable resource management, the tapped heat from an active reservoir is repeatedly reestablished by natural heat production, transmission and convection from surrounding warmer regions, and the extracted geothermal fluids are refilled by natural recharge and by injection of the depleted (cooled) fluids. Global geothermal technical capacity is comparable to global crucial energy supply in 2008. For electricity generation, the technical capacity of geothermal energy is predicted to be between 118 EJ/yr. (to 3 km depth) and 1,109 EJ/yr. (to 10 km depth). For direct thermal uses, the technical potential is predicted to range from 10

to 312 EJ/yr. The heat ejected to reach these technical capacity can be completely or partially refilled over the long term by the continental terrestrial heat flow of 315 EJ/yr. at an average flux of  $65 \text{ mW/m}^2$ . Thus, technical potential is not likely to be an obstacle to geothermal deployment (electricity and direct uses) on a global basis. Whether or not the geothermal technical potential might be a restricting factor on a regional basis depends on the availability of EGS technology (Axelsson et al., 2010). There are a lot of geothermal technologies with different levels of maturity. Geothermal energy is currently ejected using wells or other means that produce hot fluids from: a) hydrothermal reservoirs with naturally high permeability; and b) EGS-type reservoirs with artificial fluid pathways. The technology for electricity generation from hydrothermal reservoirs is mature and safe, and has been operating for more than 100 years. Technologies for direct heating making use of geothermal heat pumps (GHP) for district heating and for other applications are mature as well. Technologies for EGS are in the demo stage. Direct use delivers heating and cooling for houses including district heating, fish ponds, greenhouses, bathing, wellness and swimming pools, water purification and industrial and process heat for agricultural products and mineral drying. Geothermal resources were commercially utilized for more than a century. Today, Geothermal energy is used for base load electric generation in 24 countries, with a prediction 67.2 TWh/yr. (0.24 EJ/yr.) of supply provided in 2008 at a global average capacity factor of 74.5%; newer geothermal installations often achieve capacity factors above 90%. Geothermal energy assists more than 10% of the electricity demand in 6 countries and is utilized directly for heating and cooling in 78 countries, generating 121.7 TWh/yr. (0.44 EJ/yr.) of thermal energy in 2008, with Geothermal Heat Pumps (GHP) applications having the broadest market influence. Another source predicts global geothermal energy supply at 0.41 EJ/yr. in 2008. Environmental and social impacts from geothermal use are site and technology specific and largely manageable. Overall, geothermal technologies are ecologically useful because there is no burning process emitting carbon dioxide ( $\text{CO}_2$ ), with the only direct emissions reaching from the underground fluids in the reservoir. Historically, direct  $\text{CO}_2$  emissions were high in some instances with the full range covers from close to 0 to  $740 \text{ g CO}_2/\text{kWh}$  depending on technology design and configuration of the geothermal fluid in the underground reservoir. Direct  $\text{CO}_2$  emissions for direct use applications are unimportant and EGS power plants are likely to be modified with zero direct emissions. Life cycle

assessment (LCA) studies prediction that full lifecycle CO<sub>2</sub> equivalent emissions for geothermal energy technologies are less than 50 g CO<sub>2</sub>eq/kWhe for flash steam geothermal power plants, less than 80 g CO<sub>2</sub>eq/kWhe for projected EGS power plants, and between 14 and 202 g CO<sub>2</sub>eq/kWhth for district heating systems and GHP. Local hazards increasing from natural phenomena, such as micro-earthquakes, may be affected by the operation of geothermal fields. Induced seismic events were not been large enough to lead to human harm or relevant property damage, but proper management of this issue will be an significant step to facilitating substantial expansion of future EGS projects. Several prospects exist for technology development and innovation in geothermal systems. Technical progresses may reduce the cost of producing geothermal energy and lead to higher energy recovery, longer field and plant lifetimes, and better reliability. In exploration, research and development (R&D) is needed for hidden geothermal systems (i.e., with no surface manifestations such as hot springs and fumaroles) and for EGS prospects. Special research in drilling and well construction technology is needed to reduce the cost and increase the useful life of geothermal production facilities. EGS need innovative methods to reach sustained, commercial production rates while reducing the risk of seismic hazard. Integration of new power plants into existing power systems does not present a major challenge, but in some cases can need extending the transmission network. Geothermal-electric projects have comparatively great upfront investment costs but often have relatively low levelized costs of electricity (LCOE). Investment costs typically range between 1,800 and 5,200 per kW, but geothermal plants have low recurring ‘fuel costs’. The LCOE of power plants making use of hydrothermal resources are often competitive in today’s electricity markets, with a typical range from US cents<sub>2005</sub> 4.9 to 9.2 per kWh keep in view only the range in investment costs provided above and medium values for other input parameters; the range in LCOE across a broader array of input parameters is US cents <sub>2005</sub> 3.1 to 17 per kWh. These costs are expected to fall by about 7% by 2020. There are no actual LCOE data for EGS power plants, as EGS plants stay in the demonstration phase, but estimates of EGS costs are higher than those for hydrothermal reservoirs. The cost of geothermal energy from EGS plants is also expected to decrease by 2020 and beyond, assuming improvements in drilling technologies and success in developing well-stimulation technology. Current levelized costs of heat (LCOH) from direct uses of geothermal heat are generally competitive with market energy prices. Investment

costs vary from 50 per kWth (for uncovered pond heating) to 3,940 per kWth (for building heating). Low LCOHs for these technologies are possible because the inherent losses in heat to electricity conversion are abstained when geothermal energy is used for thermal applications. Future geothermal deployment could meet more than 3% of global electricity demand and about 5% of the global demand for heat by 2050. Indication proposes that geothermal supply could reach the upper range of projections derived from a review of about 120 energy and GHG reduction situations. With its natural thermal storage capacity, geothermal energy is especially appropriate for providing base-load power. By 2015, geothermal placement is approximately predicted to generate 122 TWhe/yr (0.44 EJ/yr.) for electricity and 224 TWhth/yr (0.8 EJ/yr.) for heat applications. In the long term (by 2050), placement forecasts based on extrapolations of longstanding historical development trends propose that geothermal might produce 1,180 TWhe/yr. (~4.3 EJ/yr.) for electricity and 2,100 TWhth/yr. (7.6 EJ/yr.) for heat, with a few countries gaining most of their main energy requirements (heating, cooling and electricity) from geothermal energy. Situation analysis proposes that carbon rule is likely to be one of the key driving issues for future geothermal development, and under the most promising climate rule situation (<440 ppm atmospheric CO<sub>2</sub> concentration level in 2100) kept in view in the energy. High-grade geothermal resources have restricted geographic distribution—both cost and technology barriers exist for the use of low-grade geothermal resources and EGS. High-grade geothermal resources are already economically competitive with market energy prices in many places. However, public and private support for research along with favorable deployment policies (drilling subsidies, targeted grants for pre-competitive research and demonstration to reduce exploration risk and the cost of EGS development) may be required to support the development of lower-grade hydrothermal resources as well as the demo and further commercialization of EGS and other geothermal resources. The effectiveness of these efforts may play a central role in establishing the magnitude of geothermal energy's contributions to long-term GHG emissions reductions (Edenhofer et al., 2012).

In 2009, electricity has been produced from traditional (hydrothermal) geothermal resources in 24 countries with an installed capacity of 10.7 GW with a yearly growth of 405 MW (3.9%) over the previous year (Bertani, 2010). The global use of

geothermal energy for power generation was 67.2 TWh/yr (0.24 EJ/yr) in 2008 (Bertani, 2010) with a global CF of 74.5%. Many developing countries are in the top 15 in geothermal electricity production (Bertani, 2010).

Conventional geothermal resources currently utilized to produce electricity are either high-temperature systems ( $>180^{\circ}\text{C}$ ), by steam power cycles (either flash or dry steam driving condensing turbines), or low to intermediate temperature ( $<180^{\circ}\text{C}$ ) by binary-cycle power plants. Around 11% of the installed capacity in the world in 2009 was formed of binary plants (Bertani, 2010).

In 2009, the world's leading geothermal producer was the USA with almost 29% of the global installed capacity. The US geothermal industry is currently growing due to state Renewable Portfolio Standards (RPS) and numerous federal subsidies and tax encourages (Huertas et al., 2010). US geothermal business is intensified mostly in western states, and only a portion of the geothermal technical potential has been developed so far (Edenhofer et al., 2012).

Presently, about 30 worldwide companies have a possession stake in at least one geothermal field. Overall, the top 20 owners of geothermal capacity control around 90% of the installed global market (Bertani, 2010). At the end of 2008, geothermal electricity conducted only about 0.3% of the total worldwide electric generation. Yet, 6 of the 24 countries shown in Figure 2.4 (El Salvador, Kenya, Philippines, Iceland, Costa Rica and New Zealand) gained more than 10% of their national electricity production from high-temperature geothermal resources (Bromley et al., 2010).

In Figure 2.4, the geothermal installed capacity by country, and overview of geothermal resources map can be seen. From the map it can be observed that major resources of the geothermal fields are in along long faults in Pacific Ocean, Atlantic Ocean. However, among onshore basins, the giant fields are in the United States.

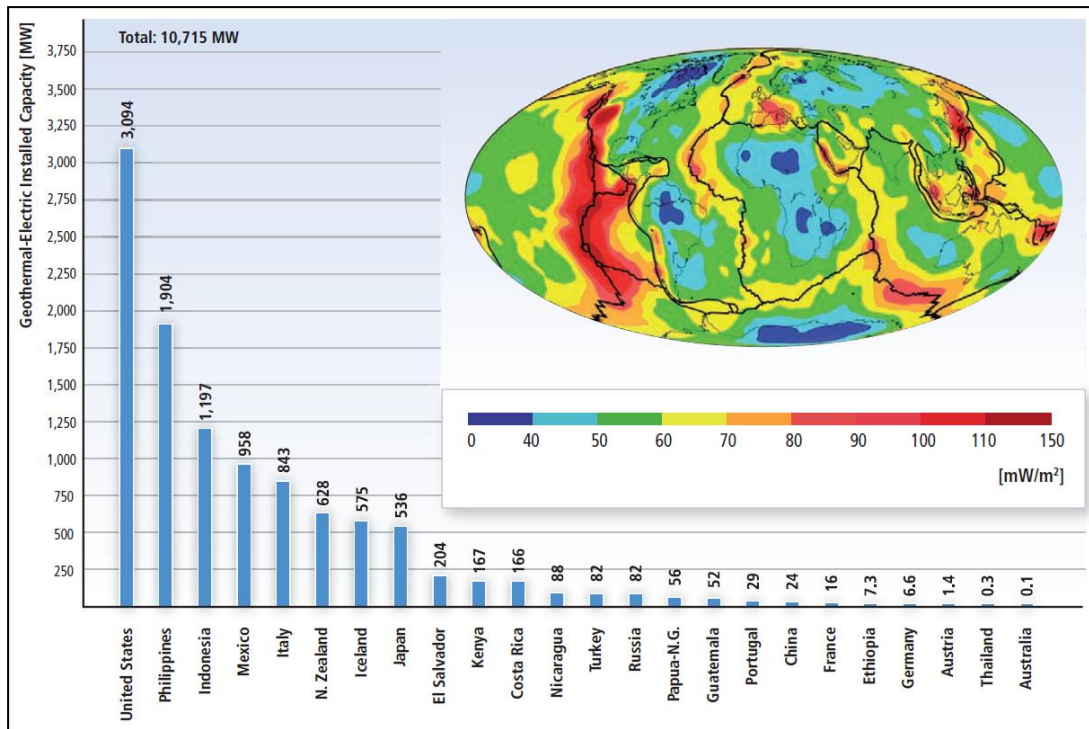


**Figure 2.4:** Geothermal electric installed capacity by country in 2009.

## 2.2 Geothermal Potential in Turkey

In Turkey, researches have recognized more than 227 geothermal fields which might be useful at the economic level and about 2,000 hot and mineral water resources (spring and well discharge and reservoir temperature) that have the temperatures ranging from 20 to 287°C (Parlaktuna et al., 2010). Until now, closely a total of 1,200 geothermal exploratory, production and injection wells were drilled in Turkey (Simsek, 2014; Dagistan, 2014). These appearances are situated mostly along the main grabens (such as Buyuk Menderes, Gediz, Dikili-Bergama, Kucuk Menderes, Edremit Grabens) throughout the Northern Anatolian Fault Zone and in the Central and Eastern Anatolia volcanic regions. The geothermal potential is projected at 31,500 MWt up to 2010 (Korkmaz et al., 2010). Furthermore, the updated prediction concerning the geothermal heat capacity potential of Turkey is intensified at 60,000 MWt geothermal heat potential (TJD, 2012). Figure 2.5 shows the main geothermal fields of western Anatolia. The installed geothermal heat capacity is 2,880 MWt for direct-use (including heat pumps) and 400 MWe for power production in Turkey, where liquid carbon dioxide and dry ice production factories are integrated to Kizildere and Salavatli power plants with a production capacity of 240,000 tons/year.



Total geothermal technical and economical electricity production capacity (hydrothermal, 0-3 km) was calculated as 2,000 MWe (16 Billion kWh/year) with the extra encouraging for 15-20 years by 15 USDcent/kWh (Mertoglu et al., 2010). The total geothermal electricity potential of Turkey (hydrothermal, 0-3 km) was calculated as 4,500 MWe (TJD, 2013).

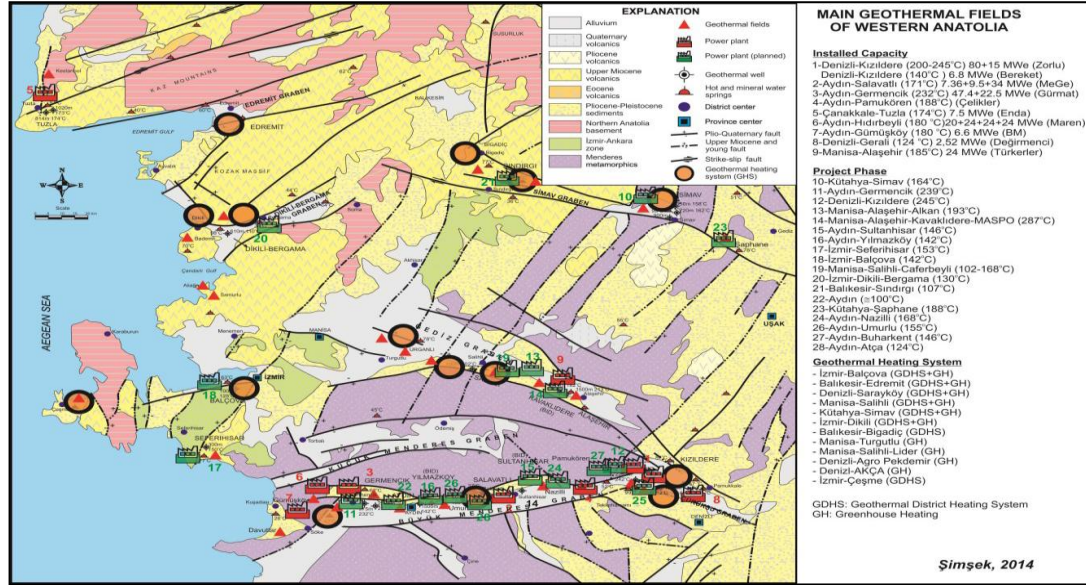


**Figure 2.5:** Main geothermal fields of Western Anatolia (Şimşek, 2014).

## 2.3 Exploration and Drilling

Meanwhile geothermal resources are subsurface, exploration methods (including geological, geochemical and geophysical surveys) were developed to find and define them. The targets of geothermal exploration are to classify and align prospective geothermal reservoirs before drilling, and to offer methods of characterizing reservoirs (including the properties of the fluids) that to allow estimates of geothermal reservoir performance and lifetime. Survey of a potential geothermal reservoir includes prediction its location, laterally extend and depth with geophysical methods and then drilling wells to test its features, diminishing the risk. All these exploration approaches might be improved (Edenhofer et al., 2012).

Reservoir engineering endeavor are focused on two aims: (a) to regulate the capacity of geothermal resource and the ideal plant size based on a number of circumstances such as maintainable use of the available resource; and (b) to guarantee safety and effective operation during the lifetime of the project. The current technique of

predicting reserves and sizing power plants is to implement reservoir simulation technology. First a notional model is established, using accessible data, and is then transformed into a numerical representation, and adjusted for make use of, early thermodynamic state of the reservoir (Grant et al., 1982).

## **2.4 Using Methods**

Every geothermal field has particular behavior of fluid in the reservoir. Moreover all has different reservoir depth and temperature gradient by depth. Each reservoir has certain permeability, and porosity of the rock parameters, that make the field either economic, or uneconomic. Economic fields are mostly have high permeable, high porosity conditions. Another factor that affects the field's situation is temperature gradient of the geothermal reservoir. Because, the temperature of the reservoir is the key factor defines method of using of the hot water. Very high temperature ( $250\text{ }^{\circ}\text{C}$ ) water has more efficiency producing energy from it. Lower temperatures sometimes are found not economically. When the engineering side of the exploration and production disciplines report the temperature of the water, it is pointed the temperature of the water when it is extracted from reservoir to the surface. Surely in every cases, the temperature will drop during traveling to the surface through pipes.

There are three methods of using geothermal sources for power plants. (1) Dry steam (2) Flash steam (3) Binary.

### **2.4.1 Dry steam**

Dry Steam Plants use hydrothermal fluids that have to be dry steam. It is most common type of geothermal technology used today. In this method, underground steam flows directly to a turbine in order to drive a generator that produces electricity. The dry steam will be directed to a turbine, which drives a generator that produces electricity. In this method desirable temperature of the underground water is greater than  $170\text{ }^{\circ}\text{C}$ . If water is hot enough, source water will reach to surface as a steam. The Geysers is the world's major only source of geothermal power. These plants emit only vapor and very negligible amounts of non-condensable gases.

For dry steam resources either atmospheric exhaust turbines or condensing steam turbines are used (Figure 2.6). New developments of Enhanced Geothermal Systems (EGS) are focusing on enhanced systems, using existing deep reservoir resources

Deep Drilling Projects (DDP) in a depth of 4 to 5 km. The aim of such projects (i.e. in Iceland and New Zealand) is the exploitation of supercritical fluid reservoirs with steam temperatures up to 400-600°C (Url-2).

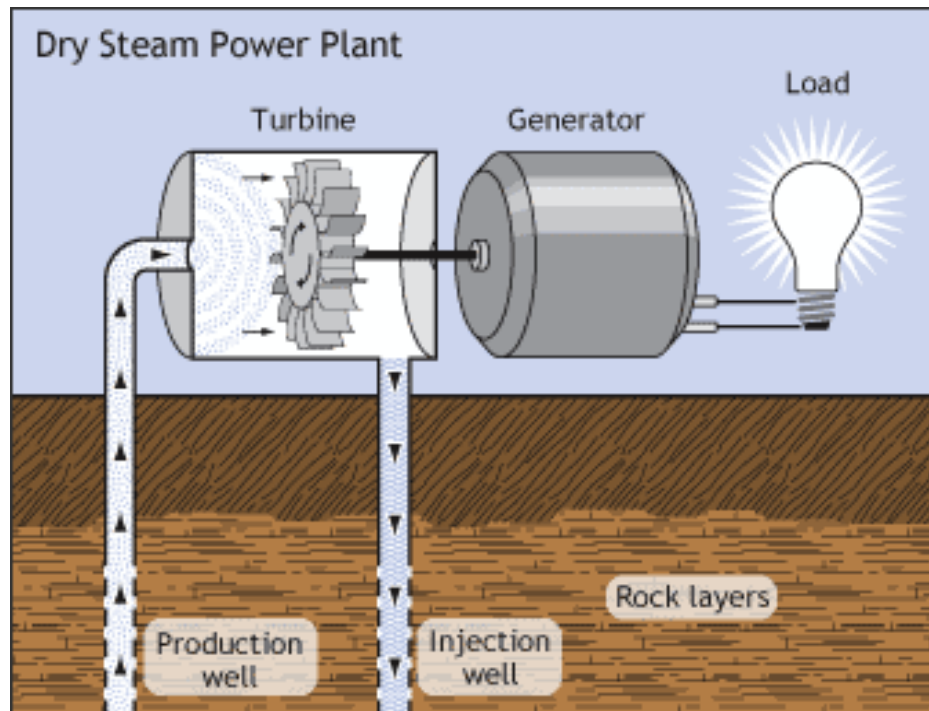


**Figure 2.6:** Dry steam method (Url-2).

Atmospheric exhaust steam turbines are straightforward. This method has advantage in terms of capital investment. With this type of plant the geothermal steam gained either straight from the wells, or subsequently flash separation that is fed through a traditional axial flow steam turbine which exhausts directly to the air (Url-2).

#### **2.4.2 Flash steam**

Fluid is sprayed into a tank held at a much lower pressure than the fluid, causing some of the fluid to rapidly vaporize, or “flash” (Url-2). Tank cools the underground water. As the water cools, it flashes, or quickly turns into vapor. The vapor drives a turbine, and powers a generator. The vapor then drives a turbine, which drives a generator (Figure 2.7). If any fluid stays in the tank, it might be flashed again in a second tank to eject more energy.

#### **2.4.3 Single flash**

In a single flash plant the fluid ruled saline steam mixture will be flashed in a separator tank beforehand the dried steam will be satisfied to the condensing steam

turbine. Condensing cycles have more supplementary tool compared to atmospheric units. This considerably rises the costs of the total plant as well as construction and installation time. Also, the occurrence of non-condensable gases in the geothermal steam, which gather in the condenser, needs the installation of a gas removal system, that will in slighter quantities emit GHG such as NO<sub>2</sub> and CO<sub>2</sub> (but in very small quantities only compared to a fossil fired power plant) (Kagel et al., 1976).

#### 2.4.4 Multiple flash

The previous sections takes into account conventional steam turbines supplied with geothermal steam gained either directly from dry steam wells, or after flash separation from wells. Though, in the case of lower enthalpy well discharge it could convert interesting to flash the separated water from the first separator tank to a lesser pressure and gain an additional Draft TNA Geothermal amount of steam, at a lesser pressure. Multi-flash systems are similar to the single-flash separately from extra flash tanks for the production of additional steam from the hot liquid coming from the separator. The steam produced during the first flash stage is sent to the first stage of the turbine, while the steam produced from the following flashes is admitted in intermediate turbine stages (Kagel et al., 1976). The decision regarding the use of a multiple flash system is a simple economic one whereby the value of the increased generation is balanced against the increased capital cost of the additional flash separation plant.

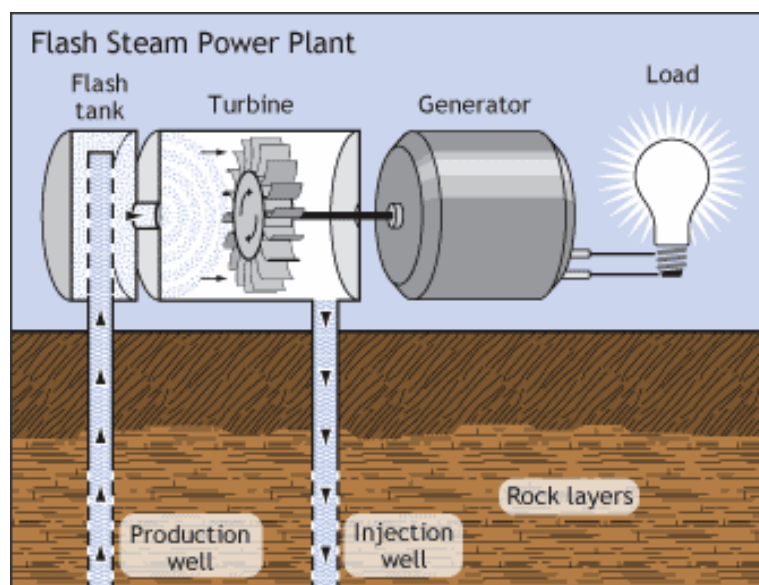


**Figure 2.7:** Flash steam method (Url-2).

### 2.4.5 Binary

Most geothermal areas have moderate-temperature fluids that below 150°C. In order to make use of the low temperature of the water, vapor cannot be used. This method works differently comparing dry steam and flash steam. Binary uses two types of fluid. Hot fluid from underground heats a second fluid, called heat transfer fluid, in a giant heat exchanger. The second fluid has a much lower boiling point than the first fluid from underground. So it flashes into a vapor at a lower temperature. When the second fluid flashes, it spins a turbine that drives a generator (Figure 2.8).

Binary technology allows the making use of the lower temperature reservoirs. Generally we can differentiate between binary method using a single fluid on the minor side of the heat exchanger or a mixture (such as a water-ammonia mixture, called Kalina technology). In an Organic Rankine Cycle (ORC) an organic working fluid vaporizes in the giant heat exchanger. The organic fluid vapor enlarges in the turbine and is then condensed in a condensing unit (alternatively, ambient air can be used for cooling) (Url-2). The condensate is driven back to the evaporator.

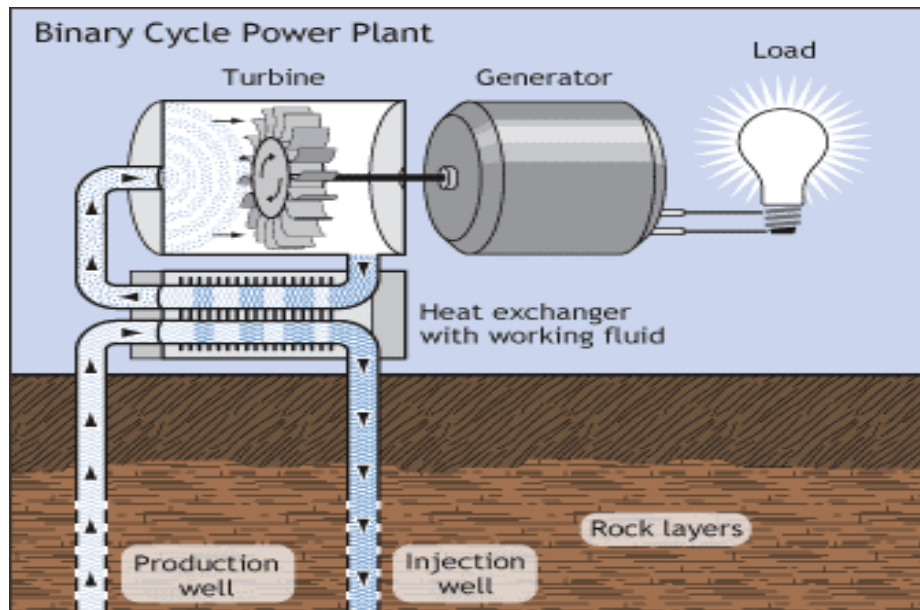


**Figure 2.8:** Binary Cycle (Url-2).



### **3. GEOLOGICAL CONDITION OF THE FIELD**

There are many counties, towns and village-sized settlements within the licensed sites and their surroundings. Some of them are, from west to east: Honaz, Bozkurt, Çardak counties and Karateke, Pınarkent, Kocabaş, Kaklık, Alikurt, Cumalı, İnceler, Beylerli, Çaltı and Gemiş towns. Denizli-Afyon highway passes directly through the Emirazizli and Kaklık licensed sites, and the near north of the Cumalı-İnceler and Çaltı-Gölcük licensed sites. In addition, the Denizli Organized Industrial Zone is located in the Emirazizli licensed site, and the Denizli Airport and a sparkling water plant are located in the near north of the Çaltı-Gölcük licensed site.

#### **3.1. General Stratigraphy of the Honaz-Kaklık Graben**

The rock groups outcropping in the Honaz-Kaklık Graben and its surroundings are categorized into six major groups according to their tectonic-stratigraphic locations, origins and rock types: the Honaz Shale (age unknown), Lycia Nappes, Dereçiftlik Group, Maymundağ Formation, Sağdere Formation, Denizli Group (pre-modern graben fill) and modern graben fill, from older to younger, respectively (Figure 3.1).

##### **3.1.1 Honaz shale**

The outcrops of the Honaz Shale are observed in the fault escarpment of the Honazdağı Horst and the raised southern foot-wall of the Honaz Fault (Koçyiğit, 2013). Most of the Honaz Shale, except a very small outcrop, is cut by the Honaz Fault (Figure 3.2) (Okay 1989). Honaz Shale is tectonically located inside the gulch of Gökdere (Gökdere Canyon), which crosses the Honazdağı Horst northward and flows into the Honaz-Kaklık Graben, and over the cover sequence of the Menderes Massif (Lycia Carbonate Nappe – 1A and 1B) and the rocks of the Paleocene-Eocene Kelkayatepe Group. Honaz Shale (named by Okay, 1989) is composed of blue-green-yellow-red- brown shale, siltstone, sandstone and quartzose conglomerate.





**Figure 3.1:** Simplified tectonic map showing the location of Turkey and its surroundings in terms of plate tectonic and important plate boundaries (Koçyiğit, 2013).



### **3.1.2 Yılanlı and Zeybekölenktepe formations**

The outcrops of the Yılanlı Formation are commonly found in the south-southwest of the Babadağ and Honaz Counties. The formation is characterized by the rudaceous, platform-type, shallow marine limestones of the cover sequence of the Menderes Massif, starting from Triassic to Late Cretaceous. Yılanlı Formation also comprises the Lycia Lower Carbonate Nappe. The outcrops of the Yılanlı Formation are also observed in the northern escarpment of the Honaz Fault in the southernmost of the Emirazizli licensed site. Yılanlı Formation is composed of gray-white, thickly-bedded, massive-structured, partly laminated, fractured, breccia, recrystallized shallow marine limestones with voids and rare gastropod content.

These characteristics make the Yılanlı Formation one of the most important rock packages forming the reservoir rock of the geothermal system in Denizli (Koçyiğit, 2013).

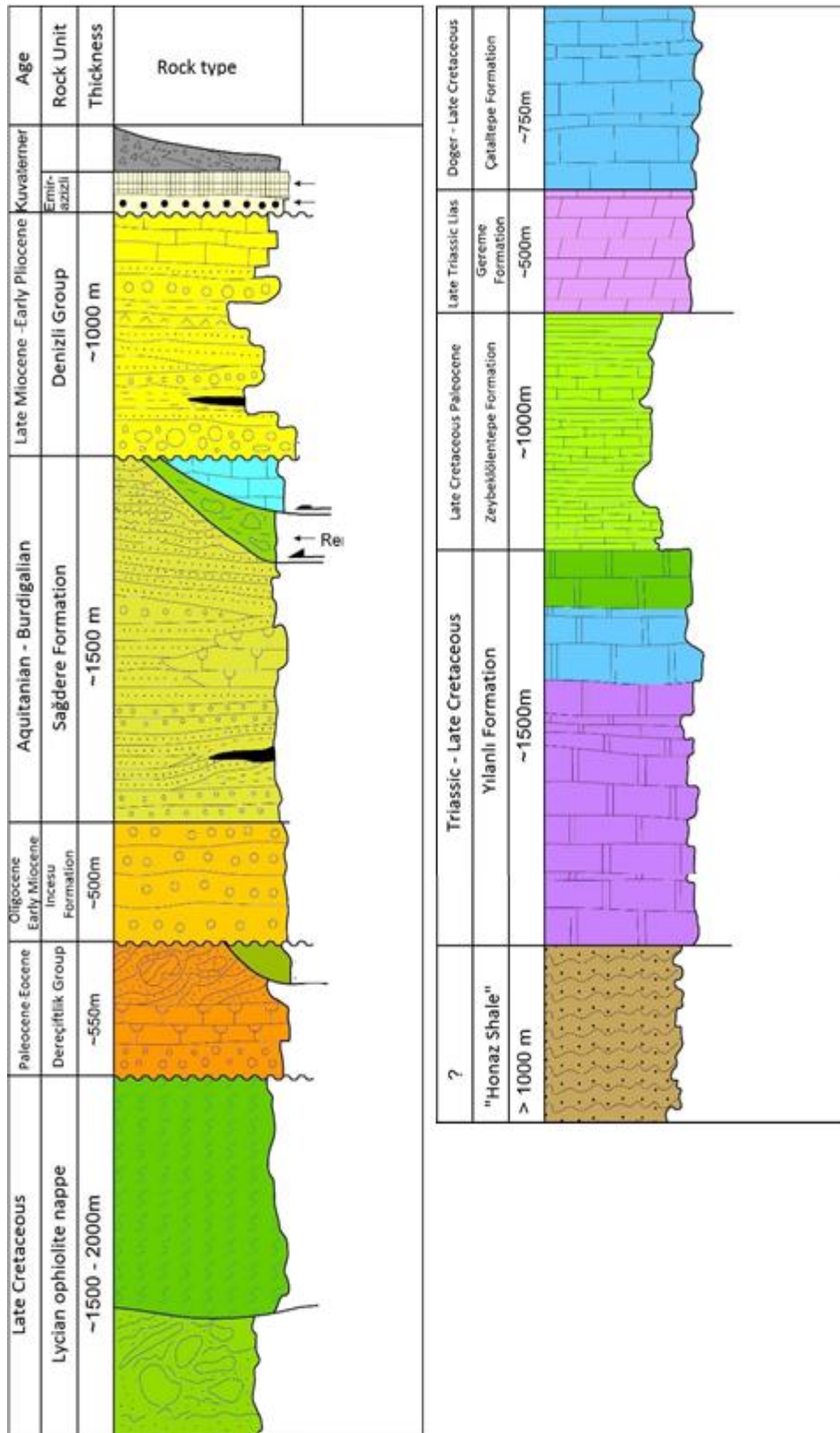


**Figure 3.2:** Generalized tectonic-stratigraphic vertical section of the Honaz-Kaklık Graben and its surroundings (Koçyiğit, 2013).

### **3.1.3 Gereme and Çatalcatepe formations**

The outcrops of the Gereme and Çatalcatepe Formations representing the Lycia Upper Carbonate Nappes are widely observed in the faulted margins of the Honaz-Kaklık and Acıgöl Grabens. The Gereme and Çatalcatepe Formations, outcropping in the north and outside the Honaz-Kaklık Graben (Çökelezdağ in the north of the Bayıralan and Baklançakırlar Villages, overlies the Late Cretaceous Lycia Ophiolite Nappe (Koçyiğit, 2013).

### **3.1.4 Dereçiftlik group**

The outcrops of lower and upper parts of the Paleocene-Eocene transgressive sequence were first observed and mapped by Sözbilir (2002) in the southern margin of the Honaz-Kaklık Graben. These, which are composed of conglomerate, reef limestone and turbiditic units, are named the “Kelkaya Formation” and “Dereçiftlik Formation”. However, the outcrops of these rock packages are observed in the surroundings of the Dereçiftlik Town (Akgün and Sözbilir, 2002). The sequence shows lithological change from red-green-yellow, heterogeneous conglomerate to reef limestones and turbidites deposited on the continental slope. The clastic sediments at the bottom of the sequence is composed of limestone, dolomite, laminated limestone, recrystallized limestone, chert, quartzite, serpentinite and peridotite derived from the Lycia Nappes (Koçyiğit, 2013).

### **3.1.5 İncesu formation**

İncesu Formation is one of the most common sedimentary sequences outcropping in the western and northern margin of the Acıgöl Graben and in the eastern, northeastern and southeastern margin of the Honaz-Kaklık Graben. The thick clastic sediments deposited in the continental, shallow marine with rapid eroding – rapid sedimentation is identified as molasses. İncesu Formation is identified as a unit representing the latest phase of the orogeny not only in the Isparta Angle but throughout the Taurus belt. The formation is typically observed in the İncesu Village located in the west of the Isparta Angle (Koçyiğit, 1983). Oligocene-Early Miocene continental – shallow marine clastic sediments, known as the “Denizli Molasse” in the literature, is also named the İncesu Formation in this study, adhering to the first naming. İncesu Formation has different contact relations with different units in the different parts of the Honaz-Kaklık and Acıgöl Grabens. İncesu Formation

uncomfortably overlies the Late Eocene sequence comprised of red conglomerate – mudstone alternation with coal bands at the bottom and nodular reef limestones in the western – northwestern side of the Acıgöl graben, whereas it is overlain by the Middle Miocene-Pliocene sequence of the stream – lake sediments with angular unconformity. In addition, the formation is cut by Çardak Fault in the northern margin of the Acıgöl Graben, and displaced more than 1 km downward in the southern hanging-wall of the fault and shows faulted contact with the Quaternary Modern Graben Fill. For this reason, it is highly possible to observe the İncesu Formation and the overlying Miocene – Quaternary Graben Fills while drilling in the northern margin and inside of the Acıgöl Graben. İncesu Formation including inter-levels of shallow marine and fossiliferous sandstone and reef limestone is aged between Early Oligocene and Early Miocene. Total apparent thickness of the unit varies from 0.5 km to 2.5 km. İncesu Formation is a secondary reservoir rock because of its coarse clastic materials and fractured structure (Koçyiğit, 1983; Şahbaz and Görmüş, 1992; Sözbilir, 2002; Koçyiğit, 2013).

### **3.1.6 Denizli group**

The sequences deposited coeval with the graben formation within the Southwestern Turkey Graben – Horst System generally, and inside the Honaz-Kaklık and Acıgöl Grabens locally, and those showing the development of the grabens are named graben fill. The Southwestern Turkey Graben – Horst System is composed of mostly two and rarely one graben fill sequence. Denizli Group, except minor details, shows outcrops within the Honaz-Kaklık and Acıgöl Grabens. The outcrops of the Denizli Group are widely observed in almost all margins of the Honaz-Kaklık Graben. Denizli Group has faulted contact with older rock packages (Koçyiğit, 2013).

Denizli Group begins with yellow-red-gray-green bottom conglomerate over the Oligocene-Miocene molasse sequence in the northern slope of the Gökpınar Creek Canyon in the southern margin of the Denizli Graben and in the upper parts of the Sarıçay Valley in the northern margin of the Honaz-Kaklık Graben, and continues upward with coarse grained sandstone, conglomerate, siltstone, mudstone and marl sequence. The bottom conglomerate is heterogeneous and shows characteristics of proximal fan deposits. The content of the conglomerate is commonly comprised of ophiolitic rocks-derived serpentinite, peridotite, diabase, chert, radiolarite and less often dolomites, recrystallized limestone, marble, quartzite and quartz, and all are

loosely bound with carbonate cement within a sandy matrix. The bottom conglomerate is conformably overlain by a thick sedimentary sequence of green marl-shale, thickly bedded and porous limestone, siltstone-mudstone, partly involving coal seams and conglomerate lenses showing characteristics of channel fill, which deposited in different environments like distal fan, braided river, flood plain, swarm and coastal. Denizli Group ends with thickly-bedded, massive-structured, porous, travertine-like limestones at the top. Denizli Group, with more than 1000 m of total apparent thickness, is Late Middle Miocene – Pliocene age according to its stratigraphic relations and mammal fossil content (Koçyiğit, 2005). Denizli Group is more loose-structured than the Oligocene and Early Miocene İncesu and Sağdere Formations because of poor diagenesis, and its coarse-grained clastic zone has high porosity (Koçyiğit, 2013). Denizli Group is both third-degree reservoir rock and the cap rock of the geothermal system in Denizli. One of the most important characteristics of the stream sediments forming Denizli Group is that the group includes many normal growth faults with net slip varying from a few centimeters to decameters. This shows that the Denizli Group is deposited in an active extensional tectonic phase coeval to the sedimentation. The outcrops of the Denizli Groups are observed in the faulted margins of the Honaz-Kaklık Graben and overlain by the Quaternary Modern Graben Fill (Koçyiğit, 2013).

### **3.2. Structural Geology and Active Tectonics**

Southwestern Turkey is divided into several grabens and horsts by different trending, seismically active normal faults, thus resulting in the development of a regional graben-horst system (Southwestern Turkey Graben-Horst System - SWTGHS). Two of the most important structures forming the GTGHS are the Honaz-Kaklık and Acıgöl Grabens, respectively (Ambraseys and Finkel, 1995). Honaz-Kaklık Graben is located in the eastern margin of W-NW trending Denizli-Çürüksu Graben, and separated by N-NW trending, E-NE dipping Şahinler Fault Zone, NE trending and NW dipping Pınarkent Fault, N-NE trending W-NW dipping Sarıçay Fault. Therefore, the bottom of the graben stays at higher altitudes relative to the Denizli-Çürüksu Graben. The first licensed sites are located in the Honaz-Kaklık Graben bounded by the Küçükmalıdağ Horst in the northeast and drained by the Eymir and Aksu Creeks. On the other hand, the second licensed sites are located in the south-

southwestern margin of the Acıgöl Graben, which is bounded by Maymundağı Horst in the north and Söğütadağı Horst in the south. A part of the graben is also occupied by the Acıgöl, where soda production continues. In conclusion, considering the neo-tectonic regimes and neo-tectonic domains, our study area is located within the Southwestern Turkey Graben-Horst System developing under the control of an extensional tectonic (Soysal et al., 1981). The most important factor having a part in the development of a geothermal system in the region is active tectonic and the structures related to it. Because active faults control the underground circulation and its geometry of both hot and cold fluids. For this reason, the active tectonic regime (extensional neo-tectonic regime) and the structures related to it (normal faults) controlling the development of the Honaz-Kaklık and Acıgöl Grabens are one of the most important issues (Koçyiğit, 2013).

### **3.2.1 Honaz fault**

Honaz Fault is an approximately 13 km long, E-W trending, W dipping, dip-slip normal fault, extending along the Honaz County and outcropping between Tütünlük Creek in the east and the Çukurbağ local in the west. Honaz Fault cuts and vertically displaces the Menderes Massif, and the Honaz Shale and Triassic-Late Cretaceous Yılanlı Formation comprising the Lycia Lower Carbonate Nappe.

Schmidt lower hemisphere projection of the slip data taken from the Honaz Fault mirror (Koçyiğit, 2013) shows that it is a dip-slip low-angle (38° dipping) detachment fault and the Honaz-Kaklık Graben extends toward N-S along the Honaz Fault. Honaz Fault is one of the important structures controlling the geothermal system in the Honaz-Kaklık Graben (Koçyiğit, 2013).

### **3.2.2 Aşağıdağdere fault zone**

Aşağıdağdere Fault Zone is a normal fault-type deformation band bounding and controlling the southern margins of the Honaz-Kaklık Graben and trending along the southern slope of the valley of the Eymir Creek in the east and the Dereçiftlik Town in the west. It is approximately 5 km wide, 10 km long. Aşağıdere Fault Zone is composed of primarily E-W, secondarily N-S trending, short (0.5-5 km), frequent, 70°N, SE and W dipping, several structural fault segments. Rock packages with different age and facieses are cut and displaced downward by the fault segments forming the Aşağıdağdere Fault Zone, thus having a faulted contact between

themselves and the Quaternary Modern Graben Fill (travertines and alluvions). Steep fault escarpment facing northward and southward, break-in-slope, crushed - breccia rock packages, fault-controlled streams, cold and hot water outlets and travertine formations parallelly aligned along the general fault trend, contact relation between pre-modern and modern graben fill, back-tilting of dropped fault block and well developed and preserved fault mirrors are important morpho-tectonic indicators proving the existence of the Aşağıdağdere Fault Zone and that some of the fault segments are geologically active (Koçyiğit, 2013).

### **3.2.3 Şahinler fault zone**

Şahinler Fault Zone is a 0.2-1 km wide, 6 km long, normal fault-type deformation zone, which bounds and controls the southwestern margin of the Honaz-Kaklık Graben. This zone also extends between the E-W trending Kaleköy Fault in the north and E-W trending, N dipping Honaz detachment fault, and forms a structural connection between these two faults. Şahinler Fault Zone is composed of primarily N-NW, secondarily E-W trending, 65°-70°E, NE and N dipping, short (0.4-4 km), frequent, several structural fault segments. Even though the Şahinler Fault Zone and its fault segments are morphologically evident, no fault mirrors related to them is observed (Koçyiğit, 2013).

### **3.2.4 Küçükmalıdağı fault zone**

Küçükmalıdağı Fault Zone is approximately 1-2 km wide, 11 km long, W-NW trending, S-SW dipping normal fault-type deformation zone, outcropping between the Yokuşbaşı Village in the east and the Acidere Ruins. Küçükmalıdağ Fault Zone, which bounds and controls the northern margin of the Honaz-Kaklık Graben and shows step-like morphology facing towards south into the graben, is composed of primarily W-NW, secondarily NE and NS trending, short (0.2-6 km), several normal fault segments. The Küçükmalıdağ Fault Zone and its fault segments exist and geologically active. The most important fault segments forming the Küçükmalıdağ Fault Zone are the Küçükmalıdağı Fault, Düzçalı Fault, Elmalı Fault, Acidere Fault and Çaykaradere Fault, from north to south, respectively (Koçyiğit, 2013).

### **3.2.5 Acidere and Elmalı fault zone**

Acidere and Elmalı Fault Segments represent the main fault of the Küçükmalıdağı Fault Zone, and define and control the northern edge of the Honaz-Kaklık Modern Graben. These two fault segments, which are located between the west - southwest of the Yokuşbaşı Village in the east and the east - southeast of the Acidere Ruins in the west, diverge from each other by 1 km N-S trending, S-E dipping fault (Koçyiğit, 2013).

### **3.2.6 Çaykaradere fault segment**

Çaykaradere Fault Segment is an approximately 4km long, NE trending,  $\sim 59^\circ$ SE dipping normal dip-slip fault. The outcrops of the fault are observed in the southeast of the Küçükmalıdağı Horst. This fault segment, with a well-preserved fault mirror, forms tectonic contact between black-blue-gray Triassic-Liassic dolomitic limestones and the Oligocene-Early Miocene İncesu Formation along its extent. Two set of overlapping fault lines are observed on the fault mirror. The older fault lines represent extensional tectonic phase, whereas the younger fault lines represents the strike-slip transpressional tectonic phase (Koçyiğit, 2013).



#### **4. FIELD STUDIES**

In this chapter, geothermal exploration work conducted between Honaz-Kaklık and Acıgöl grabens are analyzed. General geological strarigparhy and active faults in the field were investigated by the company in the licensed area. Hot water and cold water samples were taken from 22 locations in the licensed area. Analyze on the collected samples such as anion-cation analysis, heavy metal analysis were executed by the company. Consequently, a database containing pH, electric current, and petrophysical parameters was generated. The heat estimations were obtained for the target zones which were considered to be potential areas for existence of hot water in particular depth -2500 m. The target depth is defined based on geological research. The characteristics of lithology indicates porosity and permeability of certain rock groups. Denizli group contains yellow red grey green marl shale. This group considered cap rock based on its permeability. Cap rock for the reservoir regarded target depth for the field. Geothermal gradients for the regions were used to get accurate result. Heat data collected from 22 sample points were used in Geostatistical program (GS+) in order to make an estimation of temperature. As a result, more than 60,000 data points were obtained using GS+. Considering Micromine software's advantage in drawing more accurate graphics, data from Geostatistic program were used in Micromine program. The uncertainty on graphics is mentioned in the interpretation part. Field has certain water zones, and the graphic cannot be applied to all possible areas, since dominant faults were not used as a parameter in the softwares. It is intuitive that the presence of water depends on the presence of faults and their structure. For this the main investigation based on the Gravity and Magnetic study was done by the company which is very costly. New data was merged with data received from Mining softwares (GS+ and Micromine) to obtain more accurate temperature distribution. Consequently, 3 drilling target points were proposed as the main result of this thesis, and interpretation on the advantages and disadvantages of each point are provided. Overview of the investigated field can be seen in Figure 4.1.

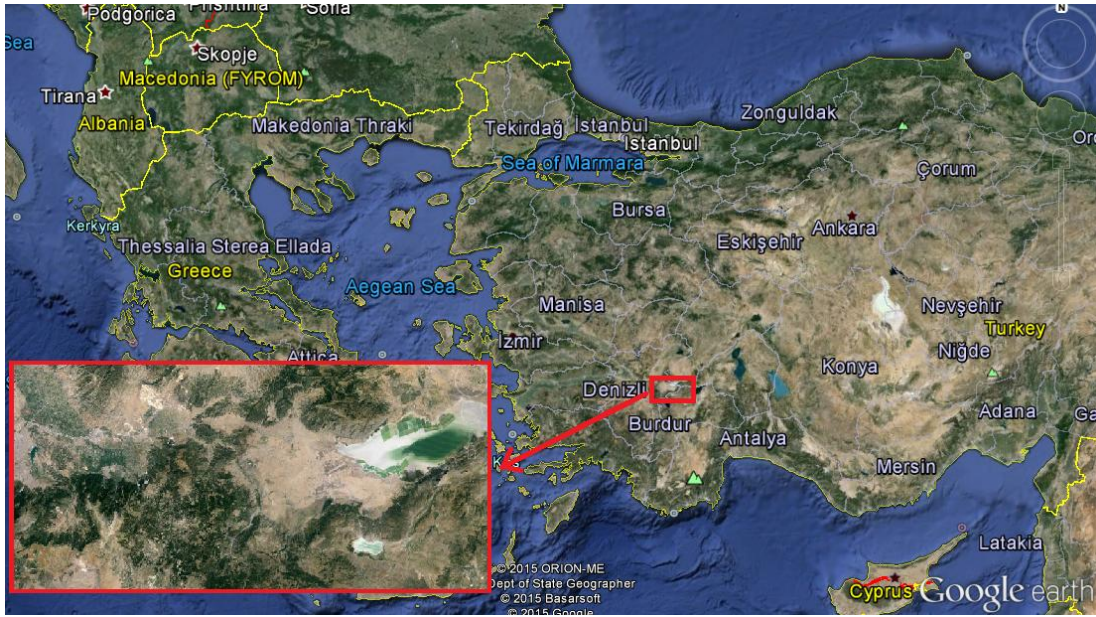


**Figure 4.1:** Overview of the investigated field.

#### 4.1 Selection of Sample Points and Their Characteristics

The samples are collected in order to reflect the geological and hydrogeological characteristics of the Promete Geothermal Co. licensed site. In addition, when selecting water sources to be sampled, the sample points which can reflect the physical and chemical properties of the waters are preferred. Therefore, it is ensured that there is no mixture into the water sources to be sampled.

#### 4.2 Hot Water Points

The data related to the hot water source is obtained from four points within the licensed site. The most important geothermal site within the licensed site is the Beylerli geothermal site. The temperature of this geothermal source is 38 °C (Table 4.1). In the first studies, it is understood that the Yandağ limestones and the Kayaköy dolomite form the source rock of the system. The geothermal site is tectonically controlled. The limestones forming the reservoir rock show highly fractured structure due to high tectonism. The units are fractured and carstic. Secondary porosity and permeability of this unit is high. Çameli Formation, which overlies the unit with angular unconformity within the study area, shows the characteristics of a cap-rock. Although the magmatic units are not observed within the study area, the former studies report the existence of hot rocks. In some studies, it is reported that the source

of high level sodium within the lake water is associated with the volcanic activity (Mutlu et al., 1999). It is understood that a 760 meters of drilling has been carried out near the Beylerli Hot Spring and the expected results have not been obtained. A new 250 meters of drilling has been carried out by Denizli Provincial Administration within the same area. It is reported that 30 °C hot water has been encountered in 100 meters deep but the water became colder deep downward. This drill yields potable water with a flow rate of 200 lt/sec. The other important source within the licensed site is the source observed in the Ilıca Neighbourhood of the Cumalı Village. However, the temperature of the water flowing from the spring to the fountain in the Neighbourhood is measured since the surface of the spring is covered. The temperature of the spring water is 27.2 °C. The spring water is tectonically controlled. The water rises to the surface through permeable conglomerates of the Çameli Formation.

Düden Spring and Kaklık Spring, of which geothermal potential are promising, is located within the licensed site. Thick travertine, which is formed by hot water sources, is located within the aforementioned areas. These two geothermal sites are also tectonically controlled. Kaklık Cave is located over an important geothermal source and on the intersection point of two faults. The cave is also abounded with water inlets. The formation and age of the travertine is studied and a new model for travertine formation is offered through geological cross-section between Pınarbaşı Spring and Kaklık Spring (Özkul et al., 2013). According to this model, as the water infiltrates deeper, it becomes warmer and rises up to the surface through discontinuity surfaces, thus forming the travertine. CO<sub>2</sub> gas, which is high in thermal waters, leads to calcite sedimentation after reaching to the surface.

It can be reported that the hot waters within this area formed at a lower temperature compared to other hot waters within the Denizli basin. According to the data obtained, it is emphasized that the water temperature drops slightly from Pleistocene to Holocene. Formation of travertine continues at the present time within the study area. Travertine pools are observed on travertine terraces. In addition, natural travertine bridges are also developed. Travertine is multicolored due to the sedimentation of materials inside the water, such as iron oxide, calcium compounds, sodium and sulphur, within the studied geothermal sites (Koçyiğit, 2013).

**Table 4.1:** Coordinates and parameters of 22 sample points of the field (Yüksel, 2013).

Number	Name	Type	X	Y	Z	pH	oC	Electric current
1	Kazanpınar	Source	695521	4183529	390	7.69	18	588
2	Göz-Kaynak	Source	697970	4183529	488	6.83	19.8	757
3	Göz-Sondaj	Drilled	697928	4183589	489	6.81	22.4	550
4	Düden Pınarı	Source	710088	4181142	569	7.68	20.4	1422
5	Kaklık	Source	709909	4192722	520	6.85	24.6	1370
6	Alikurt-Çoban Çeşme	Source	715226	4190831	587	6.66	20.7	603
7	Cumalı-Ilıca	Source	727141	4181355	881	7.02	27.2	942
8	Gemiş	Source	750482	4184553	843	6.59	20.6	767
9	Birinci Pınar	Source	752878	4186162	839	6.85	20.8	1140
10	Acı Göl	Source	760302	4191805	844	7.06	22.4	1355
11	Paşa Pınar	Source	752159	4185689	843	6.49	19.5	1166
13	Beylerli Kaplıcası	Hot Spring	736507	4178472	856	6.97	38	1299
14	DSİ Kuyu-Ova	Drilled	733249	4178486	863	7.98	19.3	332
15	Çürüksu Çayı	Drilled	698152	4188606	335	7.86	23.3	1271
16	Dereçiftlik	Drilled	706956	4187471	464	8	18.8	1051
17	İnceler	Fountain	728794	4176618	911	8.56	26.5	708
18	Sazköy	Drilled	733289	4184109	878	8.6	21.9	1389
19	Sarıkavak	Drilled	747222	4195525	869	8.44	22.4	851
20	Sarıkavak İncirlik	Source	746906	4196427	922	8.29	18.4	767
21	Çardak-Göz	Source	734833	4192089	1022	7.2	16.9	389
22	Dutluca yolu	Drilled	731593	4191232	890	7.17	19.3	746

### **4.3 Hydrochemistry**

Hydrochemistry is the science of the chemical composition of natural water and laws governing the changes in composition as a result of the chemical, physical, and biological processes occurring in the surrounding environment. Since it is the science of the chemistry of the hydrosphere, hydrochemistry is part of both hydrochemistry and hydrology.

Hydrochemistry is necessary for the development of a number of related sciences, including petrology, mineralogy, soil science, hydrogeology, and hydrobiology. Knowledge of the chemical composition of water (which determines its quality) is important for such areas of practical activity as water supply, irrigation, and fish culture. Hydrochemical data are important in evaluating the corrosion of construction materials (concrete and metal), in analyzing mineral waters, in mineral prospecting (petroleum, ore deposits, and radioactive substances), and the like. The study of chemical composition of water becomes particularly important when combating the pollution of water basins by waste water (Alekin, 1966).

Hydrogeochemistry constitutes an indispensable part of the hydrogeological studies used for determining the chemical properties and qualities of groundwaters, studying their origins, analyzing their relation with surface and rain water, solving the groundwater contamination and cleaning problems. Hydrogeochemical techniques constitute the major part of any geothermal study. They have the advantage of cheapness and rapid interpretation, especially in determining the conditions in the deep and the underground fluids, due to the development of new geothermometer techniques. Hydrogeochemical techniques also include the geochemistry of the trace ions and isotopes, the rocks and the gases. The results of the chemical laboratory analysis of the water samples and the measurements from hot and cold water sources within the Promete Geothermal Co. licensed site and its surroundings are analyzed. The results of the measurements and the chemical analysis and the hydrogeochemical properties of hot and cold waters are presented in details below.

### **4.4 Gravity and Magnetic Method**

Gravity measurements are used to determine differences in density and their lateral extent in the subsurface. These differences are usually very small and require highly

sensitive equipment to determine relative gravity anomalies. Measured data need time-dependent and static (e.g., elevation and topography) correction for local and regional conditions and are then used to conduct a contour map of Bouguer anomaly with lines of equal gravity anomaly. Positive gravity anomalies correspond to higher density subsurface. They can be of interest for geothermal exploration, as they are associated with mafic to intermediate intrusions, and geologically young intrusions (<1 Ma) can provide a potential heat source. Such structures would also commonly be detectable by a positive magnetic anomaly. Positive density anomalies can also be caused by deposition of silicates from hydrothermal activities (Milson, 2003).

Negative gravity anomalies can have several causes, some of which also have promising implications for geothermal exploration. For example, lower densities can be caused by felsic intrusions such as granites, magma bodies, higher porosities, or by highly fractured parts of a rock. Highly porous or highly fractured rocks would provide potentially interesting zones of higher fluid content and/or permeability. Alteration minerals are produced by circulation of hot water (Pedro and Jose, 2009).

Faults can also be traced by gravimetric tools, as they usually display a distinct change in density across a more or less well-defined linear zone. These faults that might have no surficial impressions can accommodate the upwelling of hot water. Gravity anomaly maps can show the extent of the sedimentary cover in basins as negative anomalies and be used to estimate the depth of the underlying basement. Such maps can provide useful first information about heat and volume of a potential geothermal reservoir. For example, gravity surveys were performed at the classic Italian site of Larderello (Fiordelisi et al., 2008), where 23,000 stations were acquired, corresponding to 1 station per kilometer, to provide subsurface structural information. 2D/3D modeling in conjunction with experimentally determined density data pointed out deep low density bodies related to molten intrusions: the potential heat source of the system (Huegnes and Patrick, 2011).

In a volcanic environment, the gravimetric differences depend strongly on the chemistry of the rocks and their porosity. Generally, solid magmatic bodies are much denser than layers of pyroclastic rocks, where densities are usually low. In highly porous rocks such as rhyolitic tuffs (where porosities can be higher than 40%), densities are also strongly influenced by the fluid content. A dry rock will be much lighter than a fluid saturated rock; steam and liquid water would also be clearly distinguishable.

Magnetic surveys measure changes of the Earth's magnetic field over time and space. The latter are associated with the composition and structure of the rock formations at the subsurface. The parameter of interest here is the magnetic susceptibility, which is a material property and can be determined and calibrated using rock samples in the laboratory. The magnetic susceptibility of rocks influences the natural magnetic field, which is measured in nanotesla (1 gamma = 1nT (nanotesla)). Measurements are performed either at the surface or airborne, if the objective is regional mapping. Various instruments can be used. The most commonly used instruments are high precision proton precession magnetometers and cesium-vapor magnetometers, which nowadays are operated together with differential GPS to record time and location accurately.

Rock magnetism is acquired when the rock forms, and it reflects the orientation of the magnetic field at the time of formation. But, rock magnetism can also change with time: if the rock is subjected to temperatures above a certain point, called the Curie temperature, it loses its magnetic properties. It is remagnetized once it cools down, now induced by the magnetic field present at the time.

The Gravity and Magnetic measurement are made for evaluation of the field situated near Denizli. The purpose of the study was to investigate the field and surrounding using Gravity and Magnetic geothermal methods considering general fault rendings, dominant faults in different depths, heating point if any, location of the hot water, and reservoir, location of the steam, the depth variation of the reservoir, and migration path of the steam to the reservoir (Huegnes and Patrick, 2011).

The owner company requested Contractor Company to carry out Gravity and Magnetic measurements which requires high cost. There are 1,726 values measured by Magnometer of the contractor company. Moreover 1,834 data measured by LaCoste&RombergGravitymeter and all data controlled by interpreter in order to make it ready for review.

Gravity and Magnetic data quality and features

Projection:

- Datum: ED-50
- Local Datum: (2m) Turkey (onshore/offshore)
- Projection model: UTM Zone 35N

#### Gravity:

- Datum: Postdam 1930
- Reduction Density: 2.30 gr/cm<sup>3</sup>
- Air Correction: 0.3086 mgal/m
- Bouguer Layer Correction: 0.04192\*ρmgal/m
- Terrain Density Adjustment : 2.30 gr/cm<sup>3</sup>
- Method and Adjustment of the Terrain Data: SRTM-90, Nagy (1996), Digital
- Latitude Correction (Gravity Theory): 1967 Sheriff
- Isostasi Correction: USGS Airyroot algorithm, Digital
- Station Measurement Range: 500m
- Profile Measurement Range: Random
- Workspace Total number of Stations: 1834
- Grid Range: 500m
- Gap Filling Range: 3000m

#### Magnetic:

- Vertical components: Direct Ground Measurement
- Workspace Total number of Stations: 1726
- Grid Range: 500m

Isostatic Gravity map (Figure 4.2) was obtained eliminating isostatic (continental) effects (Figure 4.3) on the Bouguer gravity anomalies map (Figure 4.2) wherefore commonly working in wide area. Subsequent processes are performed based on these two maps. In order to obtain information about the sub surface density from the gravity measurement, it is necessary to make several corrections to the measured value. The final corrected values of the gravity anomaly, is called Bouguer anomaly and is given in Equation 4.1

$$gc = gobs - gn + 0.3086h - 0.04193rh + TC \text{ (in mgal)} \quad (3.1)$$

where,

Gobs: Gravity readings observed at each gravity station after corrections have been applied for instrument drift and earth tides.



0.3086h: The gravity variations caused by elevation differences in the observation locations.

0.04193r h: Correction from the excess mass material between the station and sea level.

gn: normal reference gravity according to an international formula.

TC: The terrain correction accounts for variations in the observed gravitational values.

Assuming these corrections have been accurately accounted for, the variations in gravitational acceleration, the Corrected Bouguer Gravity can be assumed to be caused by variation density beneath the observation point (Url-3).

Some possible causes of density contrast and gravity anomalies in a geothermal field are: an increase of stratum density due to the mineral deposition during the geothermal fluid path; stratum alteration, faults and dykes, intrusive rock, porosity variations, and others. Most of the high temperature geothermal systems over volcanic arcs in a subduction zone setting are associated with heat transfer from a deep intrusion, which occurs at higher levels in the upper brittle crust. Culling intrusions are usually very dense bodies. Occasionally, higher gravity intrusions can be recognized by a gravity survey (Hochstein and Soenkono, 1997).

The Bouguer plate provides the simplest possible interpretational model. An easily memorized rule of thumb is that the gravity effect of a slab of material 1 km thick and 1 Mgm<sup>-3</sup> denser than its surroundings is about 400 g.u. This is true even when the upper surface of the slab is some distance below the reading points provided that the distance of the station from the nearest edge of the slab is large compared with the distance to the lower surface. The effect varies in direct proportion to both thickness and density contrast. Since topographic masses are irregularly distributed, their effects are difficult to calculate precisely and approximation is necessary. The simplest approach assumes that topography can be represented by a flat plate extending to infinity in all directions, with constant density and a thickness equal to the height of the gravity station above the reference surface. This Bouguer plate produces a gravity field equal to  $2\pi\rho Gh$ , where h is the plate thickness and  $\rho$  the density (1.1119 g.u./meter for the standard 2.67 Mgm<sup>-3</sup> density). The Bouguer effect is positive and the correction is therefore negative. Since it is only about one-

third of the size of the free-air correction, the net effect of an increase in height is a reduction in field. The combined correction is positive and equal to about 2 g.u. per meter, so elevations must be known to 5 cm to make full use of meter sensitivity (Milsom, 2003).

The gravity method is sometimes used in near-surface (uppermost  $\sim 30$  m) investigations. However, its popularity is tempered by low signal-to-noise levels and the fact that geological interpretation of high-resolution gravity data can be highly ambiguous. While the amplitudes of exploration-scale gravity anomalies are typically  $\sim 100\text{--}500$  mGal (1 mGal is roughly 1 ppm of the Earth's mean surface gravitational field), precision to less than  $\sim 10$   $\mu\text{Gal}$  (hence the term microgravity) is needed for small-scale investigations and this requires very careful fieldwork and painstaking data reduction. For example, detailed corrections for the gravity effects of individual buildings, bridges, tunnels, earthworks, and other structures should be made if the survey is conducted in a built-up area. This is additional to the standard set of corrections (Blakely, 1995) that account for larger gravity effects due to sensor drift, solar and lunar tides, Earth shape and rotation, survey elevation, local terrain, and sensor motion. Many of the near-surface applications of the traditional gravity method are related to the detection and delineation of underground void spaces such as caverns, tunnels, sinkholes, or crypts (Everett, 2013).

The high-angle, basin-bounding faults are one clear indication in the gravity gradient reaction, and simulated absent in the scalar gravity data. This is important for exploration of new geothermal systems, that faults don't have surface appearance in the geology.

Based on the report (Yüksel, 2013) the Figure 4.4 is obtained from Figure 4.3 applying correlation considering isotactic effect of the region. The interpretation was executed based on the isotactic gravity. This graphical map were drawn based on acceleration that is used extensively in the science of gravity. The measurement unit is Gal which is defined as 1 centimeter per second squared ( $1\text{ cm/s}^2$ ). The milligal (mGal) refer to one thousandth of a gal. The isotactic gravity's unit for the measurement of this field is mGal. The main purpose of using gravity method is to identify fault zones in the target depth. Hence the gravity measurement for particular depth given in Figure 4.5.

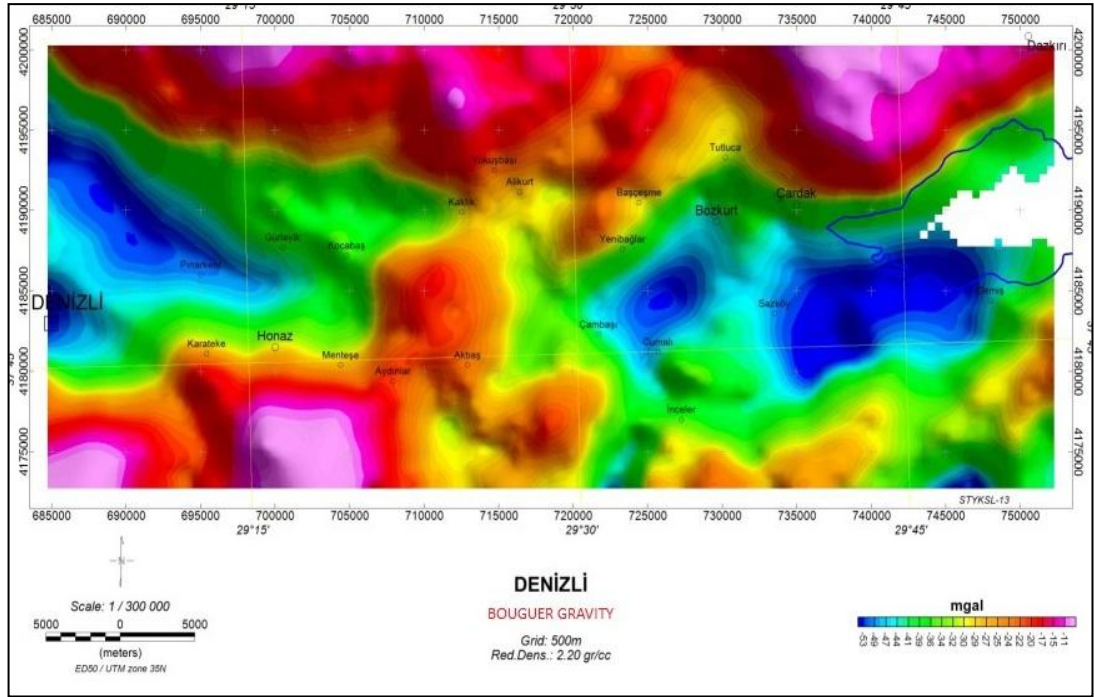


**Figure 4.2:** Bouguer Gravity (Red.Den.:2.30 g/cm<sup>3</sup>) (Yüksel, 2013).

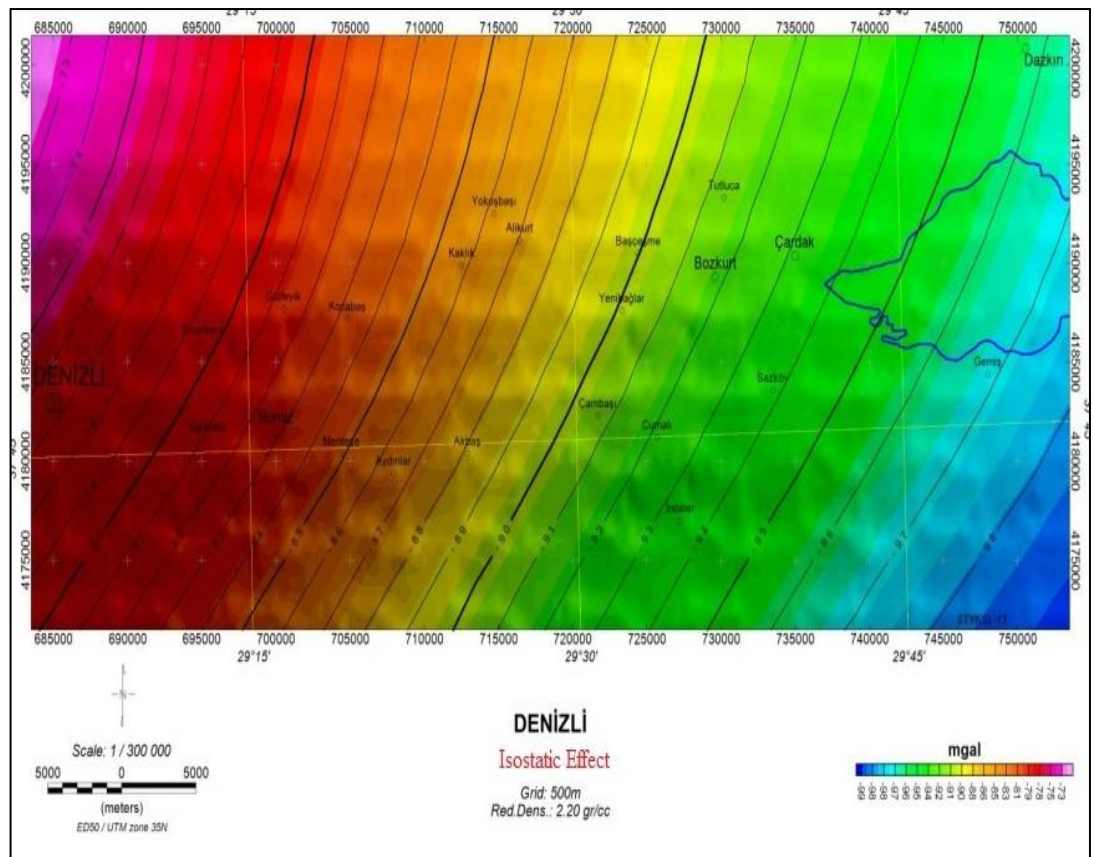


**Figure 4.3:** Isostatic effect on the field (Yüksel, 2013).

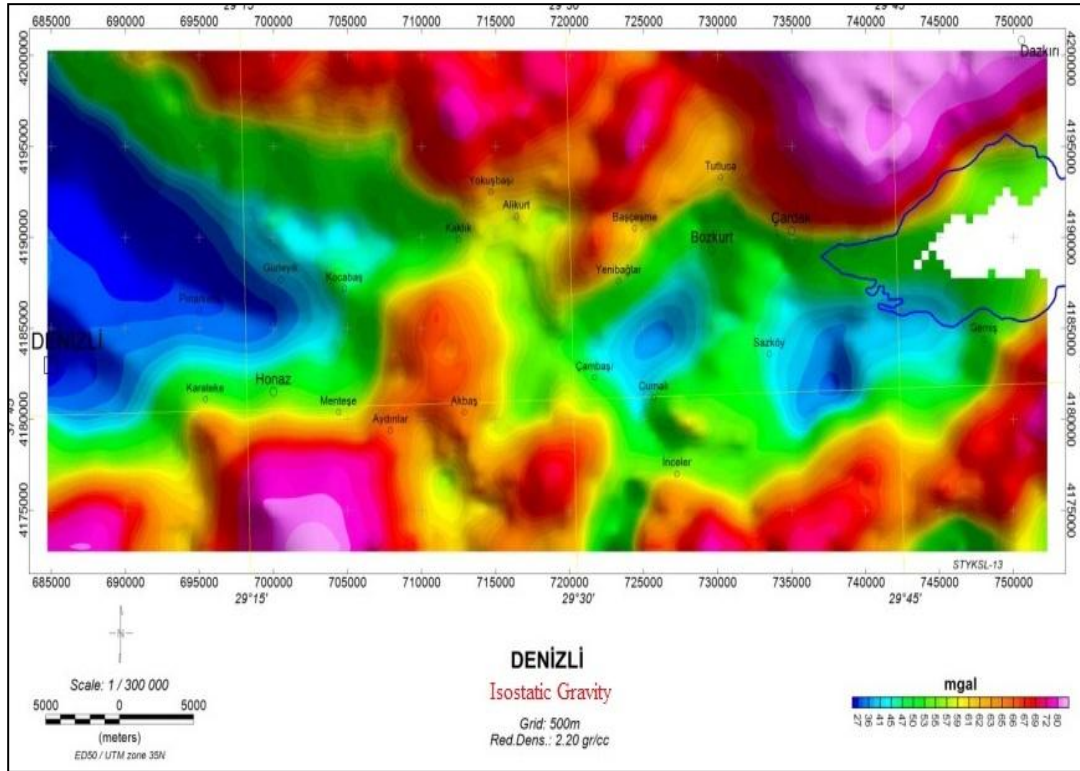


**Figure 4.4:** Isostatic Gravity of the field (Yüksel, 2013).

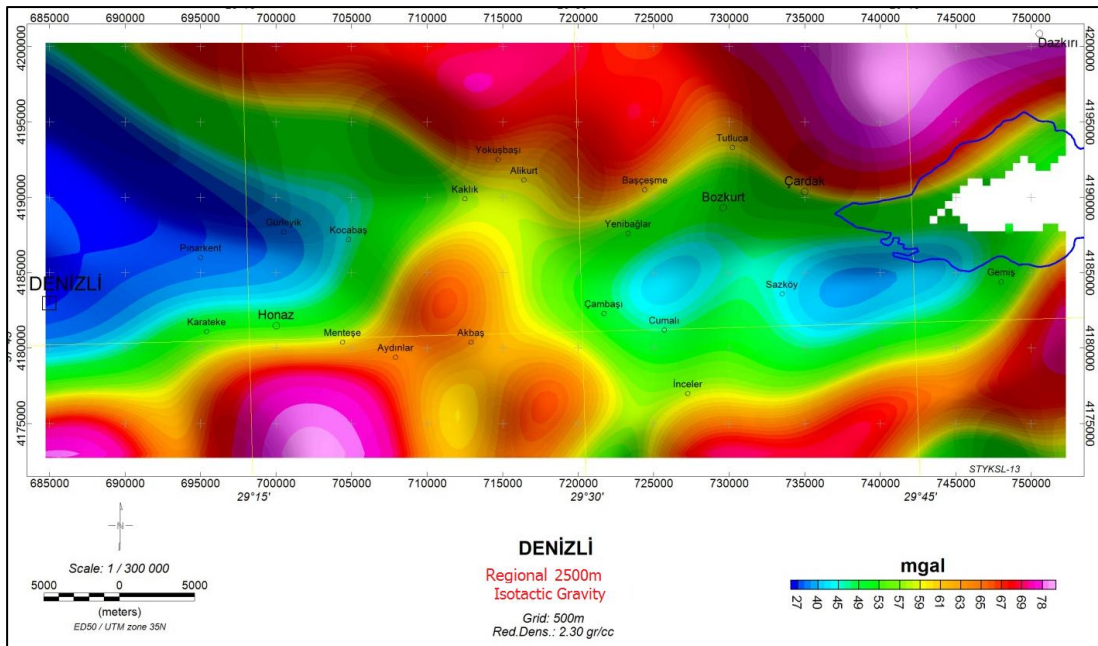


**Figure 4.5:** Gravity measurement in target depth (Yüksel, 2013).

The primary aim was to detect fault zones using gravity measurement for 2500 m depth. The fundamental principal was to specify gravity differences in the field. Sharp differences in the thin areas are the indicator for the faults. Apparently Figure 4.6 is significant evident to figure out the regional faults. It is distinct that mostly



During field application the horizontal derivatives were obtained using Residual Gravity. This method of gravity were used for 500, 1000, 1500, 2000 meter depths. After all the gradient of horizontal derivative was acquired using four data sets. It is feasible to figure out faults for any depth. It is obvious that in geothermal fields the most potential points for production are the points near the fault zones. Accordingly the fault zones were detected using magnetic methods and horizontal derivatives (Figure 4.6). During the determination of the faults, Regional faults (Figure 4.6) and Regional Dominant faults (Figure 4.7) were detected. Fault in different depths were shown in the same figure in order to make the pattern of the faults visible.

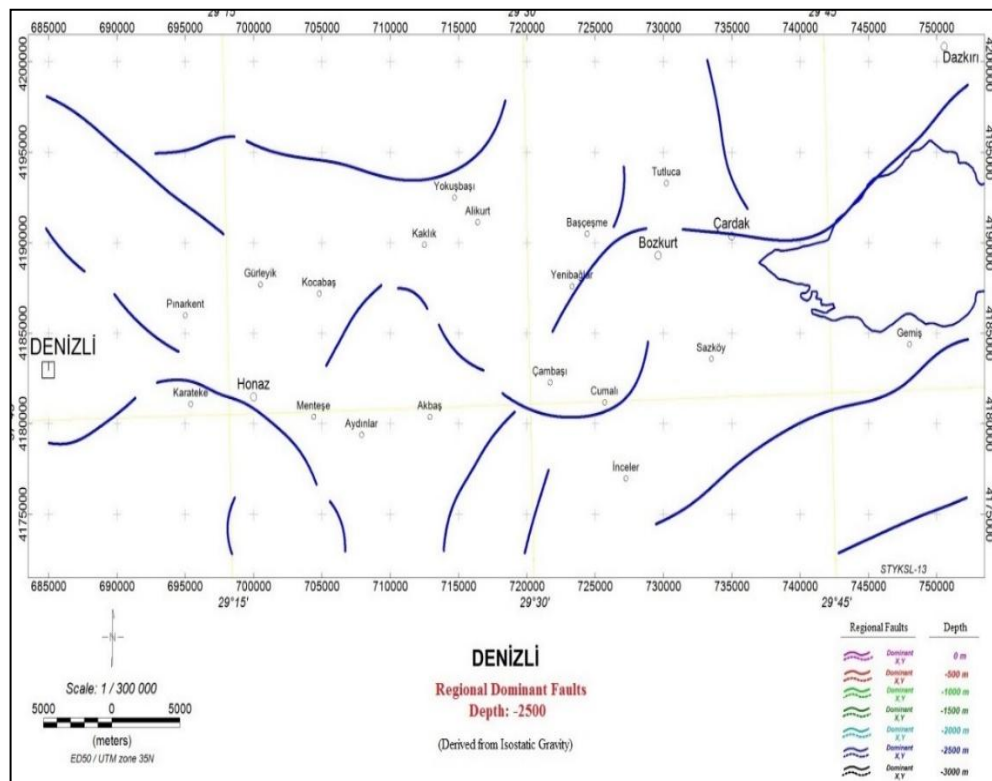


**Figure 4.6:** Regional Faults for -2500 meter depth.

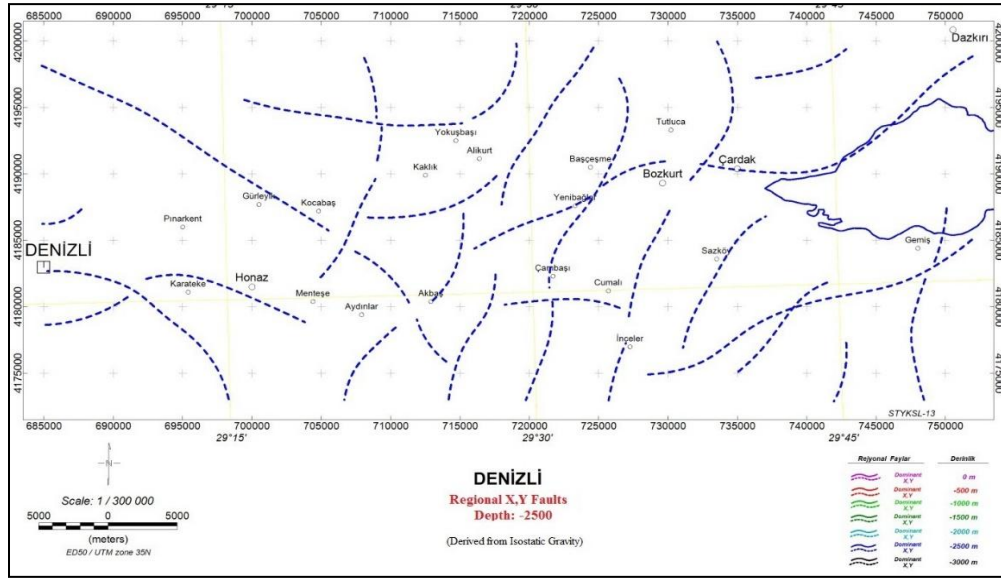


**Figure 4.7:** Regional Dominant Faults for -2500 meter depth.

Vertical Magnetic Anomalies were examined with Magnetic Analytical Signal (Figure 4.8, Figure 4.9). As a theory, dotted ellipse area should have about 150 shallow magnetic sources. However Southeastern of Bozkurt area was causing deeper sources. Rectilinear ellipse areas give an impression about magnetic alteration. Potentially low enthalpy of these areas might be an indication of water reserves.

The areas mentioned with small ellipses were considered the potential water reserves. The results were obtained using all Gravity and Magnetic tests. Generally these areas are the contained intersection of the faults, low susceptible and relatively low dense rocks. In the studied area the lack of young magmatic units, and lower magnetic amplitude than expected led to assume that the area is far away from enthalpy. Both regional and residual faults hot water can be provided to transfer. These areas can be marks of the low enthalpy reserve areas.

Additional investigation carried on to identify the water zones. Hence the data obtained from Magnetic measurement was fitted in the Gravity map in order to make accurate interpretation. Therefore, 2 graphics' crucial indications compared. The water zone indication was Gravity differences and Magnetic Anomalies behaving in a same area. Those areas considered water zones. Certainly dominant regional faults were primary aspect for pointing center of the water zones.

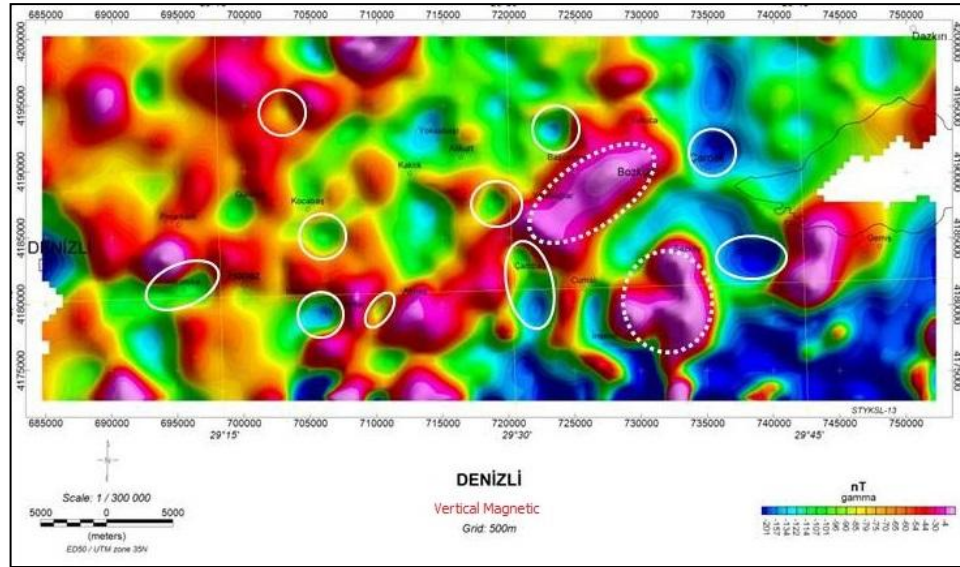


**Figure 4.8:** Vertical Magnetic intensity (Yüksel, 2013).

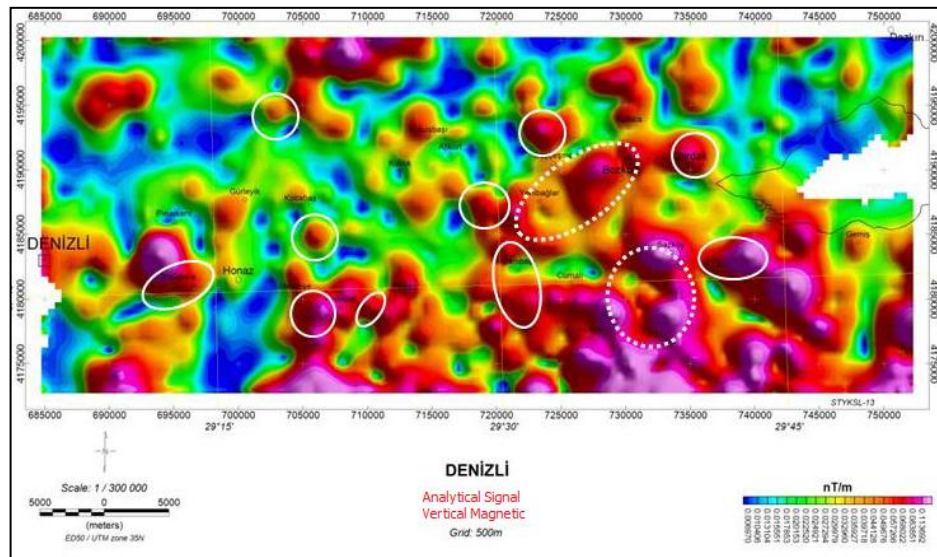


**Figure 4.9:** Analytical Signal of Vertical Magnetic (Yüksel, 2013).





## **5. SOFTWARE SOLUTIONS FOR OPTIMUM BOREHOLE POINTS**

Geostatistics is a class of statistics used to analyze and predict the values associated with spatial or spatiotemporal phenomena. It incorporates the spatial (and in some cases temporal) coordinates of the data within the analyses. Many geostatistical tools were originally developed as a practical means to describe spatial patterns and interpolate values for locations where samples were not taken. Those tools and methods have since evolved to not only provide interpolated values, but also measures of uncertainty for those values. The measurement of uncertainty is critical to informed decision making, as it provides information on the possible values (outcomes) for each location rather than just one interpolated value. Geostatistical analysis has also evolved from uni- to multivariate and offers mechanisms to incorporate secondary datasets that complement a (possibly sparse) primary variable of interest, thus allowing the construction of more accurate interpolation and uncertainty models. The mining industry uses geostatistics for several aspects of a project: initially to quantify mineral resources and evaluate the project's economic feasibility, then on a daily basis in order to decide which material is routed to the plant and which is waste, using updated information as it becomes available (Isaaks, and Srivastava, 1989)

In the working field number of data allows to make Geostatistical approach for the field. The main goal of the study is to determine the water reserves and make accurate estimation regarding temperature at particular depth. In Geostatistic Excell and GS+ programs are primary softwares used for modelling. The initial Geostatistical approach is to make a Descriptive Statistics. For this modelling Microsoft Excel is sufficient to get accurate results. As a result, the temperature is estimated for particular depth using temperature gradient for West Anatolia (Table 5.1). Away from tectonic plate boundaries, it is about 25 °C per km of depth in most of the world (Fridleifsson et al., 2008). Considering Geothermal gradient from other field in Western Anatolia, and adding somewhat pessimistic approach for beneficial

modelling 45 °C per km of depth was taken. In target depth 2500 meter, the Descriptive Statistics was implemented (Table 5.2).

**Table 5.1:** Estimation of temperature in certain depth based on geothermal gradient.

N	name	elev	tempt	0	250	500	750	1000	1250	1750	2000	2250	2500
1	Kazanpınar	390	18	26.7	32.2	37.8	43.3	48.9	54.4	65.6	71.1	76.7	82.2
2	Göz-Kaynak	488	19.8	30.6	36.2	41.8	47.3	52.9	58.4	69.5	75.1	80.6	86.2
3	Göz-Sondaj	489	22.4	33.3	38.8	44.4	49.9	55.5	61.0	72.2	77.7	83.3	88.8
4	Düden Pınarı	569	20.4	33.0	38.6	44.2	49.7	55.3	60.8	71.9	77.5	83.0	88.6
5	Kaklık Alıkurt-	520	24.6	36.2	41.7	47.3	52.8	58.4	63.9	75.0	80.6	86.2	91.7
6	Çoban çeşme	587	20.7	33.7	39.3	44.9	50.4	56.0	61.5	72.6	78.2	83.7	89.3
7	Cumalı-Ilica	881	27.2	46.8	52.3	57.9	63.4	69.0	74.6	85.7	91.2	96.8	102.3
8	Gemiş	843	20.6	39.3	44.9	50.4	56.0	61.6	67.1	78.2	83.8	89.3	94.9
9	Birinci Pınar	839	20.8	39.4	45.0	50.6	56.1	61.7	67.2	78.3	83.9	89.4	95.0
10	Acı Göl	844	22.4	41.2	46.7	52.3	57.8	63.4	68.9	80.0	85.6	91.2	96.7
11	Paşa Pınar	843	19.5	38.2	43.8	49.3	54.9	60.5	66.0	77.1	82.7	88.2	93.8
12	Gölcük Beylerli	851	26.3	45.2	50.8	56.3	61.9	67.4	73.0	84.1	89.7	95.2	100.8
13	kaplıcası	856	38	57.0	62.6	68.1	73.7	79.2	84.8	95.9	101.5	107.0	112.6
14	DSİ_kuyu	863	19.3	38.5	44.0	49.6	55.1	60.7	66.3	77.4	82.9	88.5	94.0
15	Çürüksu Çayı	335	23.3	30.7	36.3	41.9	47.4	53.0	58.5	69.6	75.2	80.7	86.3
16	Dereçifilik	464	18.8	29.1	34.7	40.2	45.8	51.3	56.9	68.0	73.6	79.1	84.7
17	İnceler	911	26.5	46.7	52.3	57.9	63.4	69.0	74.5	85.6	91.2	96.7	102.3
18	Sazköy	878	21.9	41.4	47.0	52.5	58.1	63.6	69.2	80.3	85.9	91.4	97.0
19	Sarıkavak	869	22.4	41.7	47.3	52.8	58.4	63.9	69.5	80.6	86.2	91.7	97.3
20	Sarıkavak İncirluk	922	18.4	38.9	44.4	50.0	55.6	61.1	66.7	77.8	83.3	88.9	94.4
21	Çardak-Göz Dutluca yolu	1022	16.9	39.6	45.2	50.7	56.3	61.8	67.4	78.5	84.1	89.6	95.2
22	üz.	890	19.3	39.1	44.6	50.2	55.7	61.3	66.9	78.0	83.5	89.1	94.6

**Table 5.2:** Descriptive statistic for temperature.

Mean	94.0318
Standard Error	1.46319
Median	94.5389
Mode	#N/A
Standard Deviation	6.86297
Sample Variance	47.1003
Kurtosis	1.28137
Skewness	0.65989
Range	30.3556

**Table 5.2 (continued):** Descriptive statistic  
for temperature.

Minimum	82.2222
Maximum	112.578
Sum	2068.7
Count	22

It is obvious that with this approach the ideal point to drill for starting production is the point that will be closest to maximum value in terms of temperature. Except Sum function of the Descriptive Statistics, remaining values is important during the evaluation of potential the borehole points. Apparently with 30 °C range of values, results must be deviated to the maximum.

In the kriging application set of assumption lead us to the concept of a weighted average or linear estimator, where neighboring samples are combined to provide as estimated value for the unsampled location.

The primary side of the Geostatistics is kriging. Before kriging the data used in GS+ software for checking availability of data for modelling (Figure 5.1). The most accurate Active Lag distance and Uniform interval were taken as 65,000 and 13,000, respectively.

For furtherer inception, variogram values were investigated (Figure 5.2). In this figure, most appropriate variogram model was taken. The criteria for selection is  $r^2$  which should be closer to 1.00. Despite the number of the data is extremely insufficient,  $r^2$  value for Spherical model is 0.87. Kriging helped to estimate every points' value. This allows to make 2D and 3D visual maps. Micromine software is preferable to make visual maps. The dataset which contains thousands of data obtained from GS+ software, is used in Micromine software to make useful 2D map (Figure 5.3).

In geostatistical models, sampled data is interpreted as the result of a random process. The fact that these models incorporate uncertainty in their conceptualization does not mean that the phenomenon - the forest, the aquifer, the mineral deposit - has resulted from a random process, but rather it allows one to build a methodological

basis for the spatial inference of quantities in unobserved locations, and to quantify the uncertainty associated with the estimator (Journel and Hujibregts, 1978).

A stochastic process is, in the context of this model, simply a way to approach the set of data collected from the samples. The first step in geostatistical modulation is to create a random process that best describes the set of observed data (Emery, 2005).

This approach estimating point values based on neighbor points. In this method neighbor points distance from the target point should be taking into account. The Spherical model used in kriging application represents the non-overlap of two spheres of influence. The formula is a cubic one since it represents volumes, and relies on two parameters: the range of influence (radius of the sphere) and the sill which the graph reaches at the range. In addition to these, there may be a positive intercept on the  $\gamma$  axis considered nugget effect (Equation 5.1-3) (Journel and Hujibregts, 1978).

$$\gamma(0) = 0 \quad (5.1)$$

$$\gamma(h) = C_0 + C \left[ \frac{3}{2} \frac{h}{a} - \frac{1}{2} \frac{h^3}{a^3} \right] \quad \text{when } 0 < h < a \quad (5.2)$$

$$\gamma(h) = C_0 + C \quad \text{when } h > a \quad (5.3)$$

Where  $\gamma$  is the semi-variogram and  $h$  the distance between two points of interest. The parameter  $a$  represents the range of influence of the semi-variogram. We generally interpret the range of influence as that distance beyond which pairs of sample values are unrelated.  $C$  is the sill of the Spherical component and  $C_0$  the nugget effect on the  $\gamma$  axis. You will note that the final height of the semi-variogram model is  $C_0 + C$  (Journel and Hujibregts, 1978).

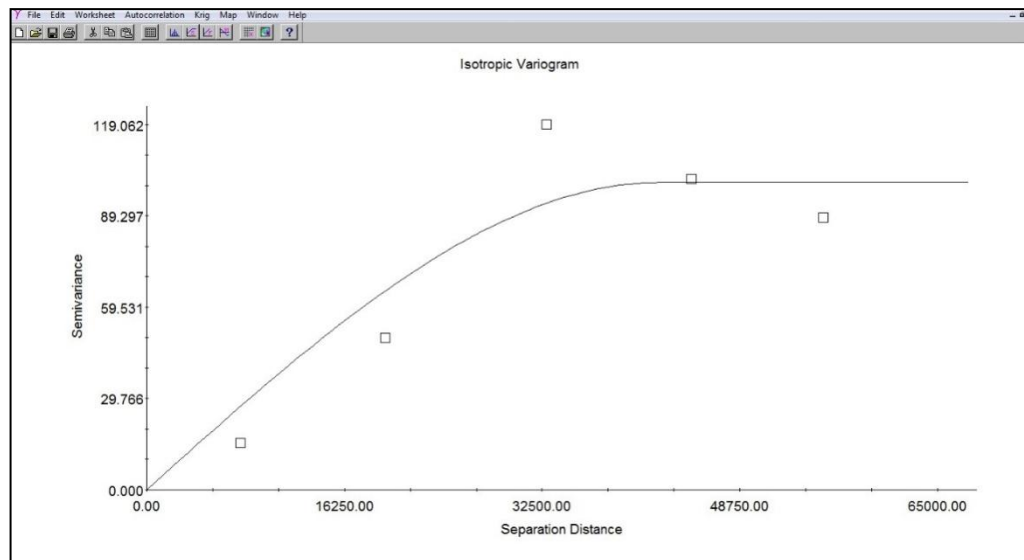


**Figure 5.1:** Variogram analysis for modelling (GS+).

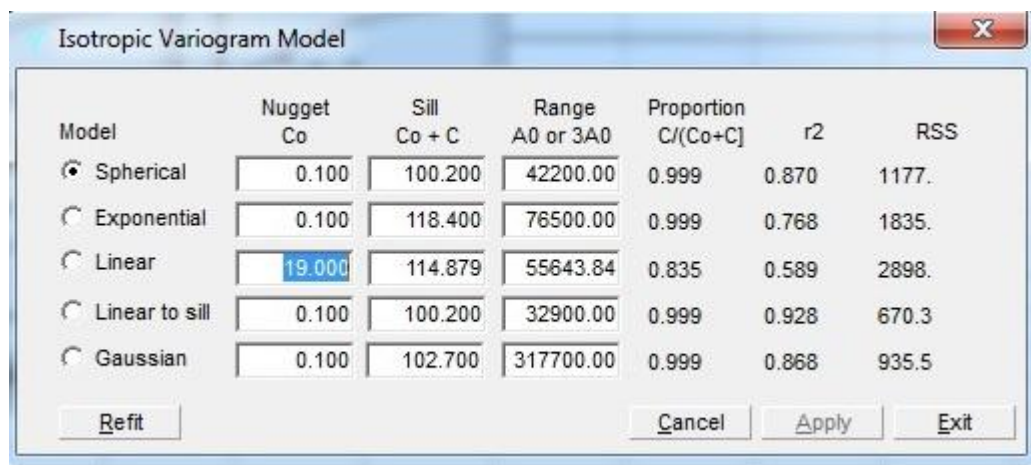


**Figure 5.2:** Variogram values and model selection. Spherical model is most suitable for the case (GS+).

The reason for using Micromine software rather than GS+ is error rate. In the GS+ software the distribution was shown to have high gaps between temperatures. This might lead to have more uncertainty with GS+. Considering that kriging has its own error, the GS+ map distribution error could make ambiguity on the final product. In order to reduce uncertainty and get more accurate result Micromine software was preferred on drawing a map. Moreover taking into the consideration of the tiny difference in the temperature could make huge difference in the production plan, the temperature differences in the legend is 1°C.

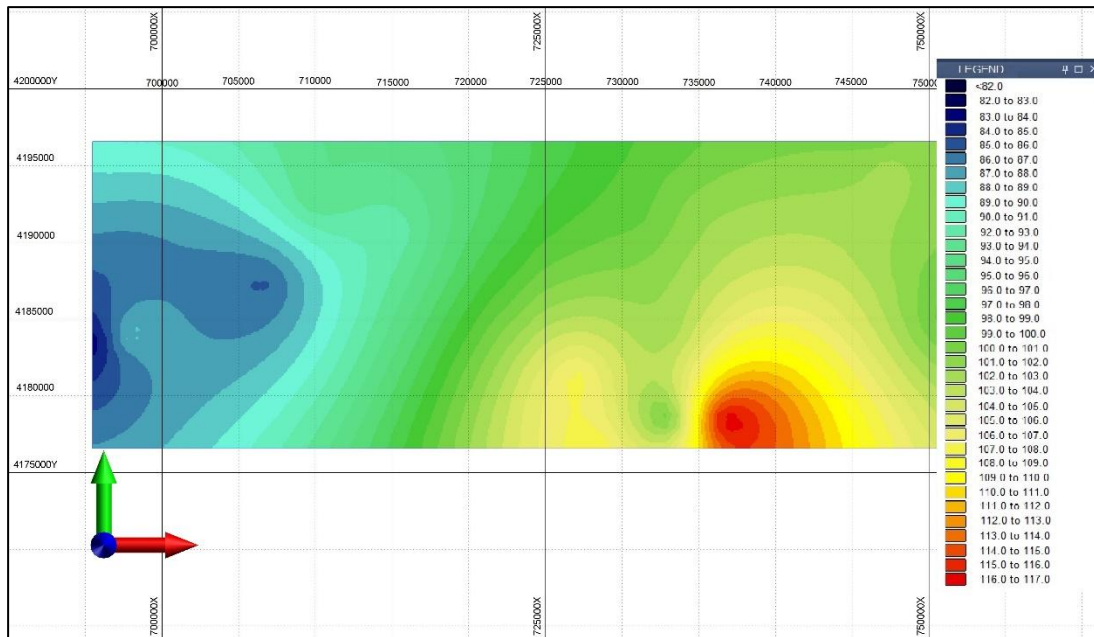


**Figure 5.3:** Heat distribution for the field. Derived from GS+ with Kriging, and visualized in Micromine software.

From the heat distribution given in Figure 5.3 is considered all field filled with water. However this is software approach according to the data inputed. Yet, the field has water zones and dry zones. Analyzing the Gravity and Magnetic, the faults were detected from gravity differences. Moreover, magnetic anomalies also indicate the water zones. The most likely water zones were identified with associating these two indicators. For instance fault zones which do not contain Magnetic anomalies were ignored. The area contains magnetic anomalies, yet there were not dominant regional faults, those were neglected as well, and considered dry zone. Additionally the fault zones and water zones were given in one graphic (Figure 5.4). As mentioned above, the outside of the circles which is considered dry zones were neglected in terms of temperature. These zones do not contain water. Apparently temperature in those areas was neglected. In the field studies, chemical and petro physical characters were mentioned. However during software solutions the only temperature parameter used to make optimum borehole suggestion. Other chemical parameters were not crucial in the first exploration stage. Furthermore, those parameters are important for production phase that might influence on selection of electric generation method. In production phase chemical characteristics give clear idea on the selection of the tools and pipes in terms of endurance, abrasion, and corrosion. There is no demand of data analysis of other parameters of water in this stage. Moreover other parameters are

used for drilling process as well. During drilling the moment drilling hits target, the potential problem might come out as blowing out. In order estimating minimum pressure and behavior parameters should be taking into account.

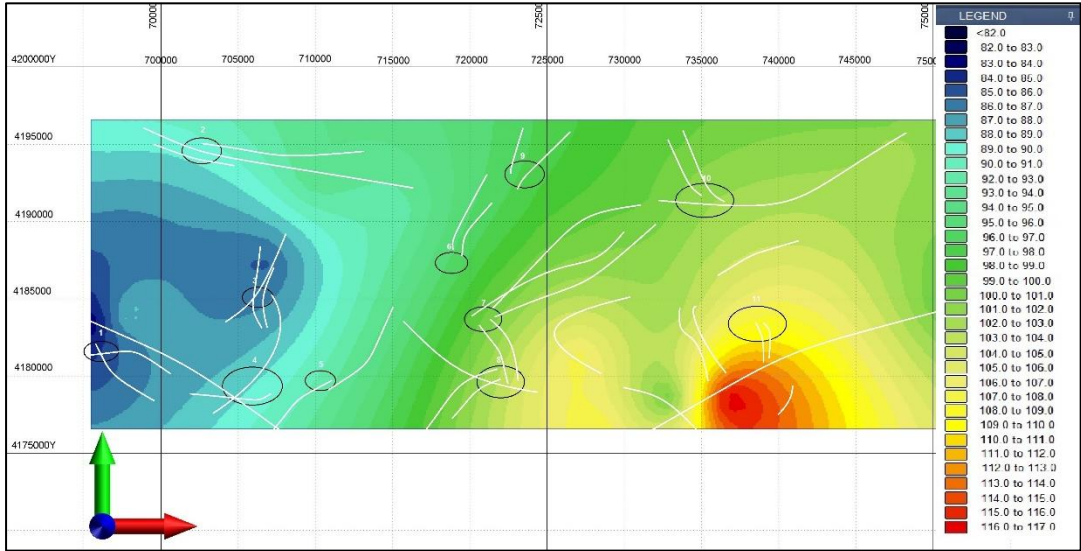


**Figure 5.4:** Water zones and faults in heat distribution map.





## 6. CONCLUSION

It is clear that this geothermal field is encouraging, and is profitable in terms of economy and sufficiency for environment. Therefore, this place was acquired by Promete Geothermal Co. and research was started. After research, the exploration phase was started. In the course of exploration few well were drilled, and different geophysical applications were implemented. Hydrogeology, Gravity and Magnetic methods were applied to the field. Certainly Magnetotellurics (MT) method is much easier to identify water zone. Nevertheless this method is very expensive for the first stage of the project. MT method cannot be convenient as a capital investment. This method is recommended to use in the second stage of the project when the reservoir requires recovery engineering.

The field was investigated with regards to geology. Including general geography, relief, rock types, primary faults were researched from different sources. Furthermore the promising points where hot water reached to the surface were analyzed. This gave to the study a hint in order to proceed the investigation. Using 22 points and regional geothermal gradient, the temperature at the target depth is obtained. Results from softwares used indicates that all field has hot water. From Gravity and Magnetic evaluation, fault zones were detected in different depths. The correlations were applied for those depths. At the end, the water zones are defined. The water zones were attached to the geothermal temperature map at 2500 meter with the help of Corel Draw software (Figure 6.1).

The outside of the circles were neglected in terms of temperature and hot water. With the help of GS+ and Micromine softwares the average temperatures were calculated for all 11 water zones (Table 6.1).

It is understandable that 3 water zones are more promising. Zone 8, Zone 10, and Zone 11 have sufficient parameters to make an interpretation. Zone 7 has a promising value on temperature gradient as well. Nonetheless, this zone has cut off value between profitable and non-profitable zones. This zone requires additional investigation. As it is mentioned in the Chapter 2 the energy generation from

geothermal field are generally based on steam. Hereby the desirable temperature is definitely more than 100 °C for the boiling temperature of the water.

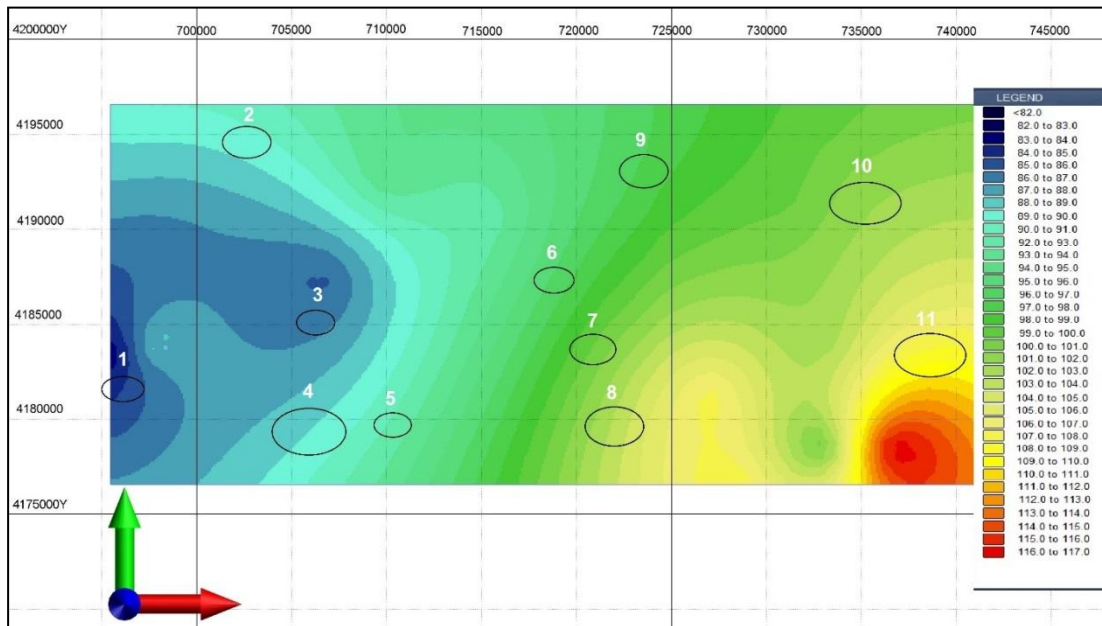


**Figure 6.1:** Merged coordinates of hot water reserves versus heat distribution of the field.

**Table 6.1 :** Average temperature and elevation of water zones

Water Zone	Average Temperature	Average Elevation
Zone 1	85	600
Zone 2	90	700
Zone 3	87	700
Zone 4	90	1200
Zone 5	92	1000
Zone 6	96	500
Zone 7	100	600
Zone 8	103	1200
Zone 9	97	1100
Zone 10	102	900
Zone 11	108.5	500

## Zone 10

This zone possesses several faults. From Magnetic and Gravity measurement, it is clear that in the target depth, possibility of presence of hot water is high. Nearest water contacts in the surface are Çardak-Göz (point 21) and Dutluca yolu üz. (point 22) sources. Both sources are inside of the water zone if vertically correlated to the 2500 meter depth. The temperature are 16.9 and 19.3 in points 21 and 22, respectively (Figure 6.2). Relying on the Gravity and Magnetic measurement and geophysical interpretation, the surface water comes from Zone 10 basin directly. This argument makes the prediction stronger about this zone. Estimated temperature at target depth is 99 °C. Presumably hot water travels vertically, and heat loss is minimum in this case. Neglecting the pessimistic approach for geothermal gradient, the real temperature in place is forecasted to be about 101 °C. One more promising side of this zone is higher EC results in the near surface points. Hot water potential increases with increment of conductivity. High conductivity signifies low resistivity. EC and resistivity are inversely proportional. Considering all relationship high EC may indicate hot water zones. Incomplete side of this approach is that it is not possible to calculate resistivity in order to calculate temperature. MT method is needed for this operation.

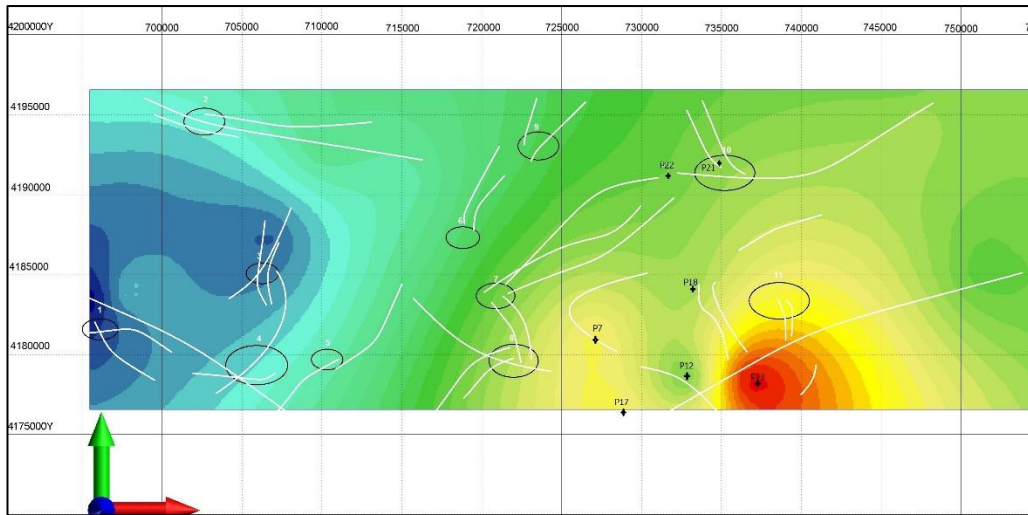


**Figure 6.2:** Nearest surface points to the water zones.

## Zone 8

This water zone is also one of the promising zones. This zone does not contain any direct contact with water reached to the surface. Nearest surface points are Cumalı-Ilıca, and Inceler points. Inceler point is only point that is fountain. However, point

coordinates are somewhat far from the basin coordinates. The interpretations were relied on totally geostatistical approach. In this zone there are four temperature zones 101 °C, 102 °C, 103 °C, 104°C. There is only very small portion for 101 °C. Considering the water path from the faults, heat loss during travel is considered high. The real temperature at 2500 meter might exceed 103 °C, and in cases of Southeast part of the water basin there is a possibility to exceed 104 °C.

### **Zone 11**

This zone is one of the largest water zone in the field. In the zone there are 107 °C, 108 °C, and 109 °C temperature values. One of the nearest points, Beylerli kaplıcası , gives a confidence to make an estimation that the source of this hot spring is Zone 11. This is the hottest water point at the surface. In this zone, faults crosses perpendicularly. This is also sufficient for production. Fault placement makes the exploration easier. Apparently hitting the target and reaching the hot water resources is much easier compared to other zones. Considering heat loss and pessimistic approach on gradient, the proper target on this zone will give an at least 107 °C temperature at 2500 meter.

For the first phase of the project, first well can be defined and drilled to start a production. Obviously, some other factors can affect the decision optimum points. Elevation is also necessary in order to set the drilling equipment and drilling rig. Furthermore maintaining this workshop for a long time leads to the financial and technical issues. Considering all factors and interpretation from the geophysical method and Geostatistical application, the optimum borehole for the first stage is decided to be on Zone 11. This zone has lowest elevation (Figure 6.3).

In order to avoid to meet dry hole it is recommended to drill to the center of the zone. The tangents of the Zone 11 are listed in Table 6.2.

The Center coordinate is derived from tangents. X axis is the same with North and South tangent, and Y ordinate is equal to Y ordinate of West and East tangent. Furthermore the center point is also the point where regional fault passes through. The center coordinate of the zone 11 is (738600: 4183400). Considering the elevation and well deviation, the total depth of the first well will be around 3.5 km.

**Table 6.2:** Optimum wellbore coordinates

	X – Latitude	Y – Longitude
North tangent	738600	4184550
South tangent	738600	4182250
West tangent	736750	4183400
East tangent	740450	4183400

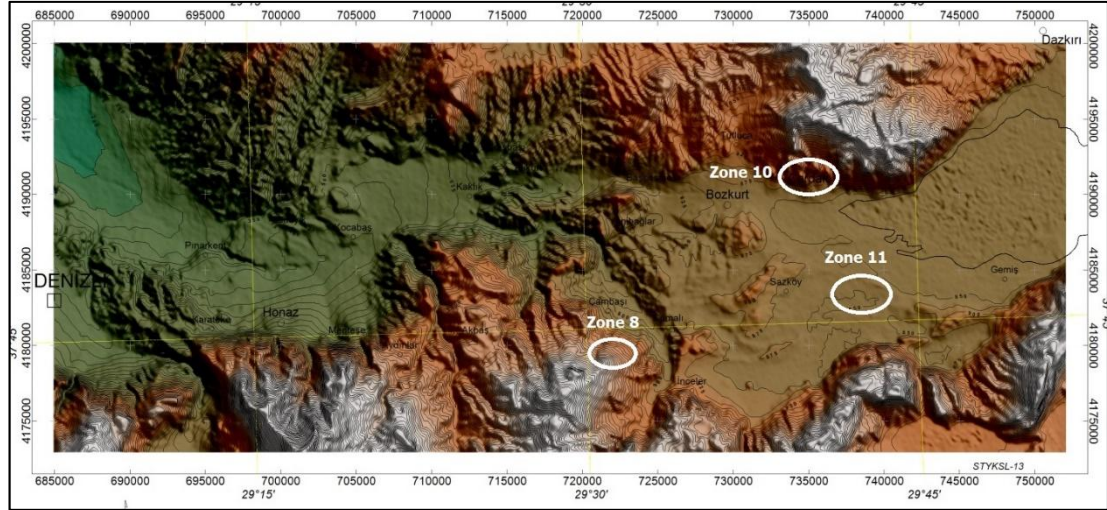


**Figure 6.3:** Suggested water zones marked on topography.



## 7. RECOMMENDATION

There is few other method to detect the hot water place in a geothermal field. However, those applications are used in petroleum industry where the profit is worth to make such investigation. Geothermal hot water and steam generally are used to generate electricity with different methods. Hot water in place is not recommended to take out and use directly. It will decrease the reservoir pressure, period of use, and temperature. That is the reason why, in geothermal power plants, circulation system is necessary to make the field life longer. Circulation is to pump the water back to the reservoir from the injection wells. Injection wells will sustain the water supply and reservoir characteristics for a long period. Yet there is a cut off temperature for injection into the wells. Extremely cold water might decrease the reservoir temperature, and damage the production plans. Produced water loses about 10 °C during travel to the surface. Water temperature decreases during generating electricity. In the last stage water should be heated before injection if the temperature is below the cut off value.

During investigation, the primary goal was to identify water reserves accurately. Gravity and Magnetic methods assisted to clarify the hot water resources in 2500 meter depth. Particularly these methods were very useful to find different fault zones in different depths. Having fault in different depths guided to have a trend lines of faults and paths for fluid. Water zones were investigated. Eventually 11 water zones are identified, and made the study to be more efficient.

Hence initial investigation was carried on. Using 22 points of surface water temperature and geothermal gradient, data was prepared for the mining programs. There were no sample from 2500 meter. Considering elevation, 3 km well is very costly. GS+ and Micromine softwares were used to estimate the temperature in every point in 2500 meter depth. Kriging method was used for modelling, and Micromine program was used for drawing a 2D map with temperature grids. Eventually, this procedure resulted in a map that contains all temperatures in every point in the field. Surely more points could lead to have more accurate modeling. It is strongly

recommended to make kriging after every well drilled in the field during project's next phases.

After first well, it is suggested to run particular well logging tools to learn reservoir's characteristics completely. Resistivity tools are very useful to identify water contact zones in particular depth. Moreover, gamma ray tools are also useful to get information about lithology in any depth. This will give sufficient data for next wells during next steps. Lithology tools would give an idea about the resistivity and sonic log errors in different zones.

In the first stage of the project uncertainty might be high. On the other hand the same study can be done for upcoming stages. Bigger data will give an opportunity to make further investigation with less error rate. Making well logging from one well will give information about few km from the borehole point. This estimation will be significant for the project for a long time.



## REFERENCES

- Akgün, F., and Sözbilir, H** (2001). A palinostratigraphic approach to the southwest Anatolian molass basin: Kale-Tavas molasse and Denizli molasses, *Geodinamica Acta*. pp. 71-93.
- Alekin, O. A.** (1966). *Khimiia okeana*. Leningrad, Soviet Union.
- Ambraseys, N. N., and Finkel, C. F.** (1995). The Seismicity of Turkey and adjacent areas. A historical Review, 1500-1800. Eren Yayıncılık, Istanbul.
- Axelsson, G.V., Bromley, C. J., Mongillo, M. A., Rybach, L.,** (2010). Sustainability task of the International Energy Agency's Geothermal Implementing Agreement. *IPCC renewable energy report. Proceeding World Geothermal Congress*. Bali, Indonesia, 25-30 April.
- Bertani, R.** (2010). Geothermal power generation in the world 2005–2010 update report. *Geothermics*. Bali, Indonesia, 25-30 April. pp. 1-29.
- Blakely, R. J.** (1995). *Potential Theory in Gravity & Magnetic Applications*. Cambridge, New York, Port Chester, Melbourne, Sydney: Cambridge University Press. Melbourne, Sydney. pp. 220-221.
- Bromley, C. J., Mongillo, M. A., Goldstein B., Hiriart G., Bertani R., Huenges E., Muraoka, H., Ragnarsson, A., Tester, J., Zui, V.** (2010). Contribution of geothermal energy to climate change mitigation. *IPCC renewable energy report. Proceeding World Geothermal Congress*. Bali, Indonesia, 25-30 April.
- Dagistan, H.** (2014). Geothermal Resource Potential of Turkey. Applications, Ssectorial Development and 2016 Projections. *US-Turkey Geothermal Workshop*. Ankara, Turkey. 21-22 October.
- Edenhofer, O., Madrugá R., Sokona, Y., Zevros, A.** (2012). *Renewable Energy Sources and Climate Change Mitigation*. Cambridge University Press. Section 3. Chapter 1-7.
- Emery, X.** (2005). Simple and ordinary multigaussian kriging for estimating recoverable reserves. *Mathematical Geology* 37.3. pp. 295-319.
- Everett, M. E.** (2013). *Near-surface applied geophysics*. Cambridge University Press.
- Fay, J. A., and Dan. S.** (2012). *Energy and the environment: Scientific and technological principles*. Chicago, Illinois, USA. pp. 11-24.
- Fridleifsson, I. B., Bertani, R., Huenges, E., Lund, J. W., Ragnarsson, A., Rybach, L.** (2002). The possible role and contribution of geothermal energy to the mitigation of climate change. *Luebeck, Germany*. pp. 59-80.

- Fridleifsson, I. B., Bertani, R., Huenges, E., Lund, J. W., Ragnarsson, A., Rybach, L.** (2008). The possible role and contribution of geothermal energy to the mitigation of climate change. *IPCC scoping meeting on renewable energy sources, proceedings*, Luebeck, Germany.
- Grant, M.A., Donaldson, I. G., Bixley, P. F.** (1982). *Geothermal Reservoir Engineering*. Academic Press, New York, NY, USA.
- Hochstein, M., and Soenkono, S.** (1997). Magnetic anomalies associated with high temperature reservoirs in the Taupo Volcanic Zone (New Zealand). pp. 1-24.
- Huegnes, E., and Patrick, L.** (2011). *Geothermal energy system: Exploration, Development, and Utilization*. Postdam, Germany. pp. 37-81.
- Huertas, D.A., Berndes, G., Holmen, M., Sparovek, G.** (2010). Sustainability certification of bioethanol: how is it perceived by Brazilian stakeholders?. *Biomass and Bioenergy*. pp. 369-384.
- Isaaks, E. H., and Srivastava, R. M.** (1989). *Applied geostatistics*. Vol 2. Oxford University Press. New York, NY, USA.
- Journel, A. G., and Hujibregts, C. J.** (1978). *Mining geostatistics*. Academic press. pp. 45-59.
- Kagel, A., Bates, D., Gawell, K.** (1976). *Geothermal Energy Association*. Washington, D.C., USA.
- Koçyiğit, A.** (1983). Hoyran gölü (Isparta Büklümü) dolayının tektoniği. *Türkiye Jeol. Kur. Bülteni* 26. pp. 1-10.
- Koçyiğit, A.** (2005). The Denizli graben-horst system and the eastern limit of western Anatolian continental extension: basin fill, structure, deformational mode, throw amount and episodic evolutionary history, SW Turkey. pp. 167-208.
- Koçyiğit, A.** (2013). Emirazizli-Kaklık, Cumalı-İnceler ve Çatlı-Gölcük (Denizli) ruhsat sahaları jeotermal potansiyelinin aktif tektonik yönden değerlendirilmesi. Orta Doğu Teknik Üniversitesi (ODTÜ) Aktif Tektonik ve Deprem Araştırma Laboratuvarları. Ankara, Turkey. pp. 13-25, 39-50.
- Korkmaz, E.D., Serpen, E., Satman, A.** (2010). Turkey's Geothermal Energy Potential. *Updated Results Proceedings of the Thirty-Fifth Workshop on geothermal Reservoir Engineering*. Stanford University, Stanford, California, USA, February 1-3.
- Kumar, S.** (2013). *Use and Capacity of Global Hydropower Increases*. Washington DC. pp. 4-6.
- Mertoglu, O., Simsek, Ş., Dagistan, H., Bakir, N., Dogdu, N.** (2010). Geothermal Country Update Report of Turkey (2005-2010). *Proceeding World Geothermal Congress*. Bali, Indonesia, 25-30 April paper #0119.
- Milsom, J.** (2003). Teachers' sense of efficacy for the formation of students' character." *Journal of Research in Character Education*. pp. 89-106.

- Mutlu, H., Kadir, S., Akbulut, A.,** (1999). Mineralogy and Water Chemistry of the Lake Acıgöl, Denizli, Turkey. *Carbonates and Evaporites*. pp. 191-199.
- Okay, A.** (1989). Denizli'nin güneyinde Menderes Masifi ve Likya naplarının Jeolojisi. MTA Bülteni. pp. 45-58.
- Özkul, M., Kele, S., Gökgöz, A., Shen, C. C., Jones, B., Baykara, M. O., Forizs, I., Nemeth, T., Chang, Y. W., Alçicek, M. C.** (2013). Comparison of the Quaternary travertine sites in the 65 Denizli extensional basin based on their depositional and geochemical data, *Sedimentary Geology*. pp. 179-204.
- Parlaktuna, M., Mertolgu, O., Simsek, S., Paksoy, H., Basarir, N.** (2013). Geothermal Country Update Report of Turkey (2010-2013). *European Geothermal Congress*. Pisa, Italy, 3-7 June.
- Pedro A. S., and Jose, A. R.** (2009). Gravity surveys contribution to geothermal exploration in El Salvador: the cases of Berlin, Ahuachapan and San Vicente areas. pp. 3-5.
- Şahbaz, A., and Görmüş, S.** (1992). Çardak (Denizli) kuzeyindeki Eosen-Oligosen yaşlı konglomeraların stratigrafik ve sedimentolojik incelemesi. *Türkiye 9. petrol Kongresi, TMMOB jeofizik Mühendisleri Odası, Türkiye Petrol Jeologları Derneği ve TMMOB Petrol Mühendisleri Odası*. Ankara, Turkey. 17-21 November. pp. 64-72.
- Şimşek, S.** (2014). Hydrogeological and isotopic survey of geothermal fields in the Büyük Menderes graben. Istanbul, Turkey. pp. 52-56.
- Soysal, H., Sipahioğlu, S., Kolçak, D., Altınok, Y.** (1981). Türkiye ve çevresinin Tarihsel Deprem Kataloğu (M.Ö. 2100-M.S. 1900) [Historical Earthquakes Catalog of Turkey and its surroundings (2100 B.C-1900 A.D.)] Tubitak Project No. TBAG-314, pp. 87.
- Sözbilir, H.** (2002). Revised stratigraphy and facies analysis of Palaeocene-Eocene supra-allochthonous sediments (Denizli, SW Turkey) and their tectonic significance. *Turkish Journal of Earth Sciences*. pp. 87-112.
- TJD, Geothermal Energy Development Report, Turkish Geothermal Association (TJD)** (2012). Ankara.
- Yüksel, S.** (2013). Gravite – Magnetik Jeotermal Değerlendirme Raporu. Denizli, Turkey.
- Url-1** <<http://waitbutwhy.com>>, date retrieved 20.04.2015.
- Url-2** <<http://mitraco-surya.com>>, date retrieved 12.05.2015.
- Url-3** <<http://waitbutwhy.com>>, date retrieved 14.05.2015.



## **CURRICULUM VITAE**



**Name Surname: Fariz Nahmatov**

**Place and Date of Birth: Baku, Azerbaijan. 12.10.1989**

**E-Mail: fariznehmetov@yahoo.com**

**EDUCATION: Baku State University**

**B.Sc.: Applied Mathematics**

### **PROFESSIONAL EXPERIENCE AND REWARDS:**

**Internship at BP Exploration Caspian Sea – 3 months internship at Drilling Engineering Department**

**Internship at SOCAR Turkiye Enerji – 1 month internship at STAR refinery project.**